

Annual Review of Biomedical Engineering

Medical Microrobots

Veronica Iacovacci,^{1,2} Eric Diller,^{3,4,5} Daniel Ahmed,⁶
and Arianna Menciassi^{1,2}

¹BioRobotics Institute, Scuola Superiore Sant'Anna, Pisa, Italy;
email: veronica.iacovacci@santannapisa.it, arianna.menciassi@santannapisa.it

²Department of Excellence Robotics & AI, Scuola Superiore Sant'Anna, Pisa, Italy

³Department of Mechanical and Industrial Engineering, University of Toronto, Toronto, Canada

⁴Robotics Institute, University of Toronto, Toronto, Canada

⁵Institute of Biomedical Engineering, University of Toronto, Toronto, Canada

⁶Acoustic Robotics Systems Lab, Institute of Robotics and Intelligent Systems, ETH Zurich, Rueschlikon, Switzerland

ANNUAL
REVIEWS **CONNECT**

www.annualreviews.org

- Download figures
- Navigate cited references
- Keyword search
- Explore related articles
- Share via email or social media

Annu. Rev. Biomed. Eng. 2024. 26:561–91

First published as a Review in Advance on
April 9, 2024

The *Annual Review of Biomedical Engineering* is
online at bioeng.annualreviews.org

<https://doi.org/10.1146/annurev-bioeng-081523-033131>

Copyright © 2024 by the author(s). This work is licensed under a Creative Commons Attribution 4.0 International License, which permits unrestricted use, distribution, and reproduction in any medium, provided the original author and source are credited. See credit lines of images or other third-party material in this article for license information.



Keywords

microrobot, targeted therapy, magnetic microrobot, ultrasound, medical imaging, minimally invasive surgery

Abstract

Scientists around the world have long aimed to produce miniature robots that can be controlled inside the human body to aid doctors in identifying and treating diseases. Such microrobots hold the potential to access hard-to-reach areas of the body through the natural lumina. Wireless access has the potential to overcome drawbacks of systemic therapy, as well as to enable completely new minimally invasive procedures. The aim of this review is fourfold: first, to provide a collection of valuable anatomical and physiological information on the target working environments together with engineering tools for the design of medical microrobots; second, to provide a comprehensive updated survey of the technological state of the art in relevant classes of medical microrobots; third, to analyze currently available tracking and closed-loop control strategies compatible with the in-body environment; and fourth, to explore the challenges still in place, to steer and inspire future research.

Contents

INTRODUCTION	562
MICROROBOTS IN THE BODY	563
Anatomy and Physiology of Key Application Areas	563
Biological Barriers	567
ACTUATION MECHANISMS	568
Magnetic Fields	569
Ultrasound	570
Light	571
Hybrid Mechanisms	573
MICROROBOT TRACKING IN VIVO	573
Ultrasound-Based Imaging	575
Magnetic Field-Based Methods	576
MICROROBOTS FOR BIOMEDICINE	577
Microrobots for the Vascular System	577
Microrobots for the Gastrointestinal Tract	580
Microrobots in Other Regions	582
OPEN CHALLENGES AND CONCLUSIONS	583

INTRODUCTION

Miniature robots for diagnosis and treatment of diseases through wireless control inside the body are becoming a reality. These miniaturized tools—in this article called microrobots—have overall or feature sizes from millimeters down to micrometers. Microrobots hold the potential to access hard-to-reach areas of the human body that would be otherwise inaccessible through traditional interventional instruments. Furthermore, in light of their controllability, microrobots can use body lumina as routes to reach specific target areas, both to overcome systemic therapy drawbacks and to enable new procedures not possible before.

While microrobots have already proved promising in lab settings, a number of challenges still need to be solved to bring such tiny machines into clinical practice. The results accomplished so far, and the physics of scaling, have taught us that the science-fiction dream of simply shrinking macroscale machines down to the microscale will not work (1). Instead, microroboticists must start from an understanding of the physics of motion, interaction, and fabrication at the microscale and utilize unique actuation and control strategies (e.g., those based on wireless actuation) to develop a bottom-up microrobotics approach (2) (**Figure 1**). Along with small device size, miniature intelligent systems designed according to this microrobotics approach are used in this article to determine what is considered a microrobot.

This article analyzes a broad set of small-scale medical devices. Existing review articles focus on either untethered submicrometer robots or on small-scale catheters/capsules/miniaturized surgical tools employing smart actuation mechanisms. Nearly two decades of research in the field, as well as fabrication and technological advancements, make it necessary to identify the concrete challenges and to identify boundaryless opportunities to cope with such challenges toward in vivo employment of medical microrobots.

This review article collects medical and technical principles intended to guide the next generation of medical microrobotics experts in the design of novel miniaturized therapeutic tools. In attempting to keep boundaries flexible, the article aims at stimulating novel hybrid actuation

Size of the target area

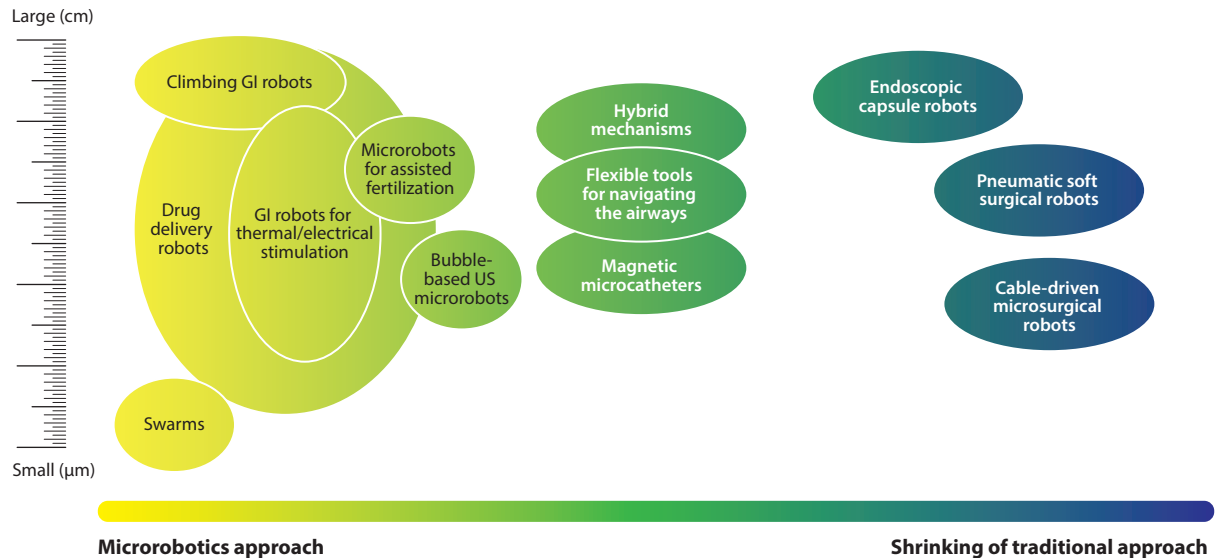


Figure 1

Classes of medical microrobots. Microrobots can be classified on the basis of both their size and the approach followed in their design—either miniaturization-driven (*right*) or using a bottom-up microrobotics approach (*left*). Abbreviations: GI, gastrointestinal; US, ultrasound.

and localization approaches and to allow application and size-oriented design of novel tools across different medical scenarios.

The aims of this article are fourfold: first, to provide a collection of anatomical and physiological information on the target working environments together with engineering tools for the design of medical microrobots; second, to provide a comprehensive updated survey of the technological state of the art in relevant classes of medical microrobots; third, to analyze currently available tracking and closed-loop control strategies compatible with the in-body environment; and fourth, to explore the challenges still in place, to steer and inspire future research.

MICROBOTS IN THE BODY

Anatomy and Physiology of Key Application Areas

The application area determines several microrobot features such as size, mechanical properties, force output, and fabrication materials. It also imposes specifications on the control strategies to be employed, for example, depending on the distance of the target from the skin and on the body region. Body lumina represent one of the likely routes for microrobot navigation. The circulatory system consisting of arteries and veins, the gastrointestinal (GI) system, the airways, the urinary ducts, the subarachnoid space in the nervous system, the eye, and the reproductive tract channel are among the main possible paths to reach a multitude of body regions (**Figure 2**, **Table 1**). Microrobots also could be eligible (at present or in the future) to dig into soft tissues or solid tumors once they have reached the surface of the target organ (3, 4).

The circulatory system. The circulatory system is an intricate network of blood vessels that enables the transportation of blood, oxygen, nutrients, hormones, and other essential substances

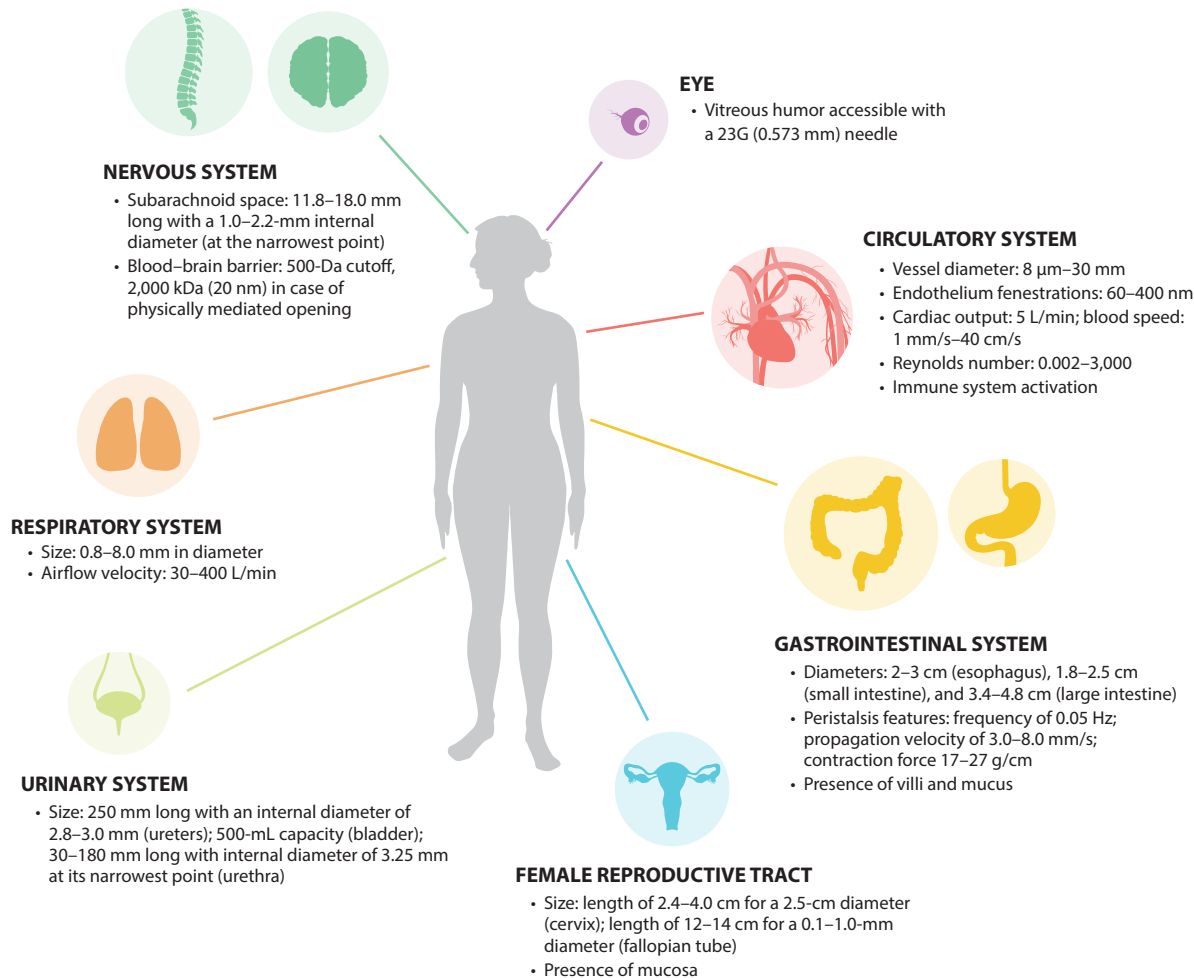


Figure 2

Overview of application areas eligible for microrobot-mediated interventions. For each area, key anatomical and physiological specifications are provided to drive the development of the next generation of medical microrobots.

throughout the body. The heart is the driver of the circulatory system, pumping blood through rhythmic contraction and relaxation with a cardiac output of 5 L/min. Blood being pumped out of the heart first enters the aorta, the largest artery of the body (diameter 25 mm, blood speed 40 cm/s). It then proceeds to divide into smaller arteries, then into arterioles, and eventually capillaries (diameter 8 μm , blood speed below 1 mm/s), where oxygen transfer occurs. The capillaries connect to venules, and the blood then travels back through the network of veins to the right heart.

The Reynolds number of blood flow, which can be used to classify the flow physics regime, ranges from approximately 3,000 to 0.0002, indicating a transition from turbulent flow in arteries to laminar flow in capillaries.

Although having many properties (density, pH, surface tension) similar to water, blood's viscosity (3.5×10^{-3} Pa s) is three times higher than water, mainly due to the corpuscular nature of the blood. Furthermore, a viscoelastic behavior of blood, induced by red blood cells, makes it

Table 1 Key anatomical features in body regions relevant to the microrobotics field

Area	Length	Diameter(s)	Features relevant to microrobotics
Circulatory system	120,000 km	8 μm (capillaries), 25–30 mm (larger arteries and veins)	Vessel endothelial fenestrations are in the range of 60–400 nm (11)
Gastrointestinal (GI) system	800 cm	2–3 cm (esophagus), 1.8–2.5 cm (small intestine), 3.4–4.8 cm (large intestine) (5)	Most of the regions of the GI tract feature villi (specific protruding structures) and a mucus layer
Urinary system	250 mm (ureters); 30–40 mm (female)/ 180 mm (male) (urethra)	2.8–3.0 mm (ureters), 3.25 mm (urethra at narrowest point)	The ureter enters the bladder wall at an oblique angle to prevent backflow of urine to the kidneys
Subarachnoid space	11.8–18.0 mm (narrowest segment) (12)	1.0–2.2 mm (internal diameter at narrowest point)	Canal occlusions are tolerable below 30%; a few structures (between 1 and 3 mm, depending on the population segment) are eligible for navigation in the subarachnoid space (10)
Eye	NA	NA	The vitreous humor is an aqueous viscoelastic gel typically removed (through vitrectomy) to allow retinal access; the eye is transparent to light; ocular injections with up to 23G (0.573 mm) needles are acceptable (13)
Reproductive tract (female)	2.4–4.0 cm (cervix), 10 cm (extrauterine part of the fallopian tube), 2–3 cm (tubal isthmus)	2.5 cm (cervix), 0.1–1.0 mm (tubal isthmus) (14, 15)	The mucosa typically has three to six primary folds and is surrounded by a firm and thick muscular wall
Respiratory system	Starts in upper respiratory tract (nasal cavity to larynx) and ends in lower respiratory tract (lungs down to alveoli)	0.8–8.0 mm (airways)	Airflow typically can be approximated to laminar with some exceptions—e.g., in the nose and the larynx—where turbulence causes inhaled particles to be thrown out of the airstream or contributes to the production of sound, respectively

Abbreviation: NA, not applicable.

necessary to consider it as a non-Newtonian fluid. This is relevant when understanding the dynamics of a microrobot moving in the circulatory system. On top of that, blood is not transparent to visible light, thus making traditional endoscopic visualization solutions impossible.

The gastrointestinal system. The human GI tract is a series of multilayered, tubular organs that extend from the oral cavity through the esophagus, the stomach, and the small and large intestines and terminate at the anus. The esophagus and the intestine are collapsed muscular tubes (5), while the stomach is a dilated and J-shaped organ with two openings (esophageal and duodenal) and five major regions.

Each part of the GI tract has a distinct mechanism of motility. The food bolus is transferred to the distal part of the stomach with the help of tonic contractions, which last from several minutes to several hours. In the distal part of the stomach, peristaltic muscular contractions are initiated by spontaneous electrical waves (5). These contraction waves feature a frequency of $2.83 \pm 0.35 \text{ min}^{-1}$ and a propagation velocity of 3.0–8.0 mm/s (6).

In the intestine, two motion patterns can be identified: segmentation and peristalsis. Segmentation, reaching rates of up to 12 contractions/min in the duodenum, is intended for mixing and

is caused by consecutive contraction and relaxation cycles. Peristalsis is the process of moving chyme through the intestinal tract from the stomach to the colon by means of a series of muscle contractions acting in a wave pattern (1–2 cm/min). Peristalsis results from circumferential and longitudinal muscle contractions, with forces of 26.9 g/cm in the longitudinal direction and 17.2 g/cm in the circumferential direction (7, 8).

The respiratory system. The primary function of the respiratory system is to deliver oxygen to and remove carbon dioxide from the blood. Air is delivered into the lungs through a series of conducting airways that connect the external air to the alveoli where gas exchange with blood takes place.

Breathing—also known as ventilation—is the movement of air across the conducting airways between the atmosphere and the lungs. Air motion is caused by pressure gradients that are produced by contraction of the diaphragm and thoracic muscles. Under normal conditions, the average adult takes 12 to 15 breaths (a full cycle of inhalation and exhalation) per minute. The respiratory pump of the lungs is versatile, capable of increasing its output 25-fold, from a normal resting level of approximately 6 L/min to 150 L/min in adults.

Other regions. Other possible body regions that may be accessible noninvasively through medical microrobots are briefly described below.

The urinary system. The urinary system includes two kidneys, the bladder, two ureters, and the urethra. The density and viscosity of urine are similar to those of water. The bladder is an elastic muscular sac capable of holding 500 mL of urine. The connections from the kidneys to the bladder, known as the ureters, enter the bladder at an oblique angle to prevent back flow of urine into the kidneys.

The subarachnoid space. The subarachnoid space is a fluid-filled space in the brain and the spinal cord, which together constitute the central nervous system. The cerebral ventricular system is made up of four ventricles: two lateral (one in each cerebral hemisphere), one in the diencephalon, and a fourth in the hindbrain. Inferiorly, it is continuous with the central canal of the spinal cord. The subarachnoid space is filled with cerebrospinal fluid (9), through which brain access by microrobots could be granted, thus overcoming the limitations and invasiveness associated with craniotomy and skull-associated access procedures. Microrobots between 1–3 mm (depending on the population segment) could be safely navigated through the cerebral spinal fluid without occluding more than 30% of the canal flow. Such access to the central nervous system proved safe with endoscopes (10).

The eye. The eye contains two fluid chambers, namely, the aqueous humor—between the cornea and iris—and the vitreous humor—between the lens and retina. The latter appears particularly interesting as it allows access to the retina, a crucial yet hard-to-reach area of the eye.

The female reproductive tract. The female reproductive tract includes the vagina, the uterus, and the fallopian tubes. The vagina allows for sexual intercourse and childbirth, and it is connected to the uterus at the cervix. The uterus accommodates the embryo during pregnancy, which develops into the fetus. The uterus also produces secretions that help the transit of sperm to the fallopian tubes, where sperm fertilizes egg cells produced by the ovaries. The cervix allows access to the fallopian tubes, which are particularly intriguing in the field of microrobotics for the applications of assisted fertilization and zygote transfer.

Biological Barriers

A primary biological barrier of the human body is the skin, which is typically incised during surgery to access the internal organs; still other barriers are present inside the body, such as the mucus layers in the GI and genitourinary tracts or the blood–brain barrier (BBB). To be effective in medical applications, microrobots may need to be engineered with stealth capabilities that allow them to evade the body's immune systems and with the ability to overcome this range of biological barriers. With realization of these capabilities, microrobots would offer a promising solution for accessing previously inaccessible regions, both by navigating into the lumina and by crossing the lumen wall. The role played by biological barriers may also vary on the basis of the pathological state of the target region.

Immune system. Numerous microrobots operating at the microscale require meticulous consideration of their interaction with the immune system. When microrobots are introduced into the body, the immune system perceives them as foreign entities and initiates a response depending on microrobot size, shape, surface properties, and materials used. The interaction between immune cells and microrobots (if they are larger than 0.5 μm) can elicit various immune responses, such as phagocytosis (16), where macrophages (a type of white blood cells) recognize and engulf the microrobots for removal from the body. Macrophages exhibit the ability to execute phagocytosis of larger foreign particles, even those with dimensions comparable to or larger than numerous microrobots, typically from 10 to 100 μm in size (17). While the time for phagocytosis may vary on the basis of microparticle size, composition, surface properties, and the immune response to foreign material, it is essential to note that the process can take several minutes to hours (18, 19). Microroboticists are currently developing stealth microrobots with surface modifications to prevent labeling the microrobots for recognition by immune cells and actively suppress immune cell recognition, to mitigate the immune reaction toward these particles (17).

The impact of a disease on the immune system varies depending on several factors, including the specific disease type, its stage, the overall health status of the patient, and the chosen therapy. Microrobots can trigger immune responses, potentially generating antibodies that limit their effectiveness. In certain medical conditions, such as cancer, the phenomenon known as the enhanced permeability and retention effect could become advantageous (20). This effect facilitates the accumulation of microparticles at the target site, primarily due to the presence of leaky blood vessels in the affected area. However, the interplay between disease, the immune system, and microrobots remains poorly understood, necessitating further research in this area. Understanding these variations is crucial for effective microrobot deployment in disease treatment and management.

Mucus barriers. On the other hand, if microrobots have to cross a biological barrier protected by a mucus layer, this layer should be deeply characterized and accounted for.

Mucus layer alterations can occur in pathological conditions, thus changing the requirements for microrobots to work effectively. Mucus in the airways can undergo significant hypersecretion and thickening in diseased conditions such as asthma (21). In the GI system, both thickening and depletion could be witnessed when passing from cystic fibrosis (22) to ulcerative colitis (23), to mention a few widespread pathological states. These variations should be taken into account in microrobot design as playing a pivotal role in microrobot locomotion across a duct and therapeutics penetration across a cavity's epithelium.

The blood–brain barrier. The BBB serves as a protective shield, blocking harmful substances from entering the brain through the bloodstream while still allowing essential nutrients and molecules to pass. It plays a critical role in maintaining homeostasis within the brain by

meticulously controlling the transfer of substances between the blood and brain tissue. The BBB is composed of specialized endothelial cells that line the blood vessels in the brain, as well as supportive cells such as astrocytes and pericytes. One of the significant challenges associated with the BBB is its ability to limit the passage of therapeutic drugs into the brain.

The tight junctions between the endothelial cells create a physical barrier that limits the diffusion of large molecules, including many drugs, from the bloodstream into the brain tissue. The intricate nature of the brain and the challenges associated with accessing it present significant obstacles to the study and treatment of brain diseases. Small molecules below 500 Da, including polar substances (glucose, amino acids, organic ions, and nucleosides) and lipophilic compounds (barbiturates, ethanol, and caffeine), can passively diffuse through the BBB (24). However, for larger molecules approximately 2,000 kDa (~20 nm) in size, external stimulation such as high-intensity focused ultrasound (HIFU) is required to facilitate their transport across the BBB (25). While current microrobotics systems are still relatively large in terms of penetrating the BBB, advancements can be made by designing them in such a way that drug-loaded microrobots, under external stimulation, could temporarily open up the barrier and facilitate the transport of larger drug molecules. It is important to note that the BBB can become more permeable or get damaged in various neurodegenerative diseases and pathological conditions (26). Performing careful control experiments is essential for studying the opening of the diseased BBB using microrobots and to ensure effective delivery of drugs.

ACTUATION MECHANISMS

The selection of a proper actuation mechanism for a microrobot must be performed while keeping in mind the features of the working environment (presence of fluid, environmental forces to be withstood, dimensional constraints, biological barriers) and the properties of the microrobot itself. A primary challenge in microrobot actuation is how to find a proper compromise between miniaturization, physical scaling laws, and production of a sufficient output force. Furthermore, despite some traditional actuation strategies (e.g., pneumatic actuators or cable-driven mechanisms) being used successfully in miniaturized surgical tools (27, 28), the presence of cables and pipes limits the number of degrees of freedom and make it challenging to get to certain hard-to-reach areas of the human body due to the presence of tethers (for actuation or powering). As shown in **Figure 3**, in this review we focus on actuation mechanisms based on magnetic field, ultrasound (US), and light, which allow the powering of untethered devices and represent a microrobotics approach, as proposed in the Introduction.

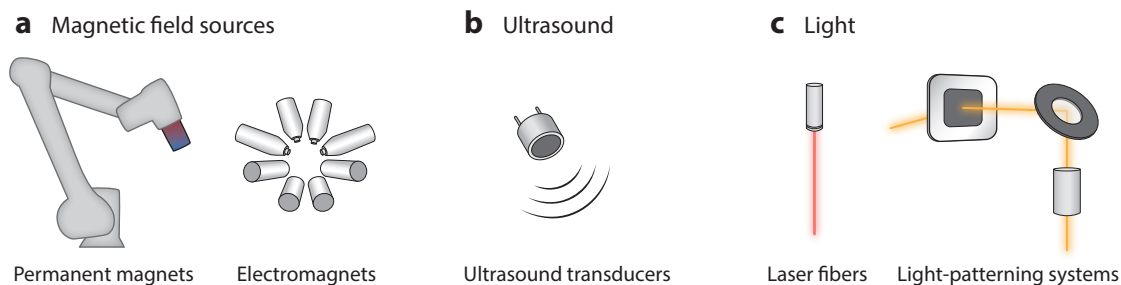


Figure 3

Overview of the wireless actuation mechanisms effective in medical microrobotics: (a) magnetic fields, (b) ultrasound, and (c) light. For each method, common field sources examples are depicted.

Magnetic Fields

An actuation method that has become widely used in microrobotics is the magnetic field (29). Magnetic fields are one of the elective choices when one is willing to exert a force on or produce navigation of small-scale objects within the body in a safe and highly controllable way. Here, we present an overview of the basic physics principles behind magnetic actuations, the advantages of using such a strategy, the platforms developed so far to implement magnetic control, and the challenges still in place in magnetic actuation.

Overview and advantages. By placing magnetic material on board a microrobot for use inside the body, a field generated from outside can exert forces and torques directly on the device without onboard powering sources or cables and tethers. By controlling the current through a set of electromagnets [or the pose (position and orientation) of a large external permanent magnet], a magnetic microrobot can be controlled precisely and quickly. Soft (nonpermanent) magnetic materials offer good biocompatibility and can be scaled down to the nanometer size, while hard (permanent) magnet materials offer magnetic programmability, which can result in tunable sophisticated actuation of flexible or multilink microrobots. In the first case, an external magnetic field produces the magnetization of the microrobot and the creation of a magnetic link intended to produce force. In the latter, the internal magnet will be induced to align with the applied field in three dimensions, like a compass needle, and will be pulled toward regions of high field strength. Workspaces of a few to tens of centimeters can be easily achieved, while projecting fields over the whole human body can be done only by moving magnets or by using very large source systems. Magnetic fields at low frequency permeate air and bodily tissues in the same way, so modeling of magnetic actuation is a tractable problem that translates readily from the lab to in vivo settings (30).

Large collections of thousands to millions of micrometer-scale soft-magnetic particles can be controlled as a cohesive swarm by a rotating magnetic field. The field rotation induces a fluidic vortex pushing particles apart, where the magnetization of the particles holds the swarm together, leading to a swarm whose size and shape can be modulated on demand by the field frequency, magnitude, and other parameters. Such swarms can encapsulate cargoes and navigate through extremely small openings and lumina (31).

Field generation. Magnetic fields are generated by permanent magnets or by electromagnetic coils (**Figure 3a**). Electromagnets allow for fast and conveniently controllable generation of magnetic fields. Electromagnets with tens to thousands of turns and coil currents up to tens of amperes can induce magnetic fields over different areas of the human body. While machines such as clinical magnetic resonance imaging (MRI) systems can generate several teslas of magnetic flux density using superconducting magnets, electromagnets that can be quickly switched for robotic control to generate fields of tens to hundreds of milliteslas and field gradients from tens to thousands of milliteslas per meter. Special arrangements of electromagnets such as nested Helmholtz coils can create uniform fields over a large area (while imposing severe geometric constraints on the workspace) (32). Electromagnet systems for microrobotics consist of two to eight individual coils, where more coils give more control over the components of the magnetic field to allow for full state control of the actuated internal magnet (33). More open-workspace arrangements of coils possibly combined with position control systems (e.g., linear stage or robotic arms) create nonuniform field distributions but are more suitable for medical use (34, 35).

Fields can also be generated using large permanent magnets, typically made from NdFeB (a rare earth materials alloy that is strong and nearly impervious to demagnetization). To control the field, permanent magnets can be rotated in place (36) or translated and rotated with one (37) or

two robotic arms (38). Permanent magnets to generate fields inside the human body have a typical size of a few centimeters to tens of centimeters and a weight of several kilograms (39).

Challenges. Field generation systems for medical use typically create a nonuniform field distribution. As a consequence, information on precise position and heading of onboard magnets is typically required to exert a precise magnetic force and torque and reduce instability conditions. This also requires precise calibration of the field over the operational space, which is nontrivial but a solvable problem (40).

For many medical applications (especially at the submillimeter scale), achievable magnetic forces are weaker than desired. This is especially true for areas deep within the body, as magnetic field magnitudes fall off very quickly with distance from the generation source (the field is roughly proportional to $1/\text{distance}^3$). While in principle larger magnetic fields can always be generated from larger magnets or driving electromagnets with more current, in practice a field strength of tens of milliteslas is the limit for medical-scale systems due to heat generation in electromagnets, with several hundred milliteslas being an upper limit where most magnets become demagnetized (41).

Ultrasound

In recent years, US has emerged as a promising modality for the actuation of medical microrobots. US demonstrates prospects for wirelessly navigating microrobots in medical applications, owing to its capacity to safely penetrate deep into tissues and produce substantial propulsive forces. Here, we present an overview of US-based microrobots, discussing their advantages and the challenges they currently face.

Overview and advantages. US is a type of mechanical or longitudinal wave that travels through a medium by inducing vibrations in the particles of the medium. US-activated microrobots are an emerging technology that has primarily been studied in controlled 2D and 3D environments (42, 43). Acoustically activated microswimmers in the initial research phase are primarily influenced by bulk acoustic streaming and a standing wave field, shaped by the boundaries of the resonating acoustic chamber (44).

Normally, standing acoustic wave fields are generated within controlled experimental setups with precisely defined boundary conditions. However, when transitioning to in vivo experimental conditions, establishing a standing wave field becomes highly challenging due to the complex and arbitrary 3D nature of areas of the body. As a result, there is a need to develop traveling-based microrobots, as acoustic waves interact exclusively with microrobots without being constrained by the boundary conditions of the workspace (45). Stable microbubbles, confined within hydrogel containers (~ 10 to $200\ \mu\text{m}$), can oscillate when irradiated with US, generating thrust through the combined effects of radiation and streaming forces (42, 43, 46, 47). While these systems can generate relatively large propulsive forces (ranging from nano- to micronewtons), ensuring the stability of the microbubbles and achieving precise navigation has proven to be extremely challenging. Therefore, researchers are actively developing new actuation mechanisms that depend on stable oscillating polymeric appendages. For microrobot steering, magnetic materials are quite straightforward to utilize (43, 48), as mentioned above. However, developing a US-based steering strategy will be crucial to develop a simple, robust, and compact manipulation approach (49). Currently, there is growing enthusiasm for developing self-assembled US microrobots utilizing clinically approved microbubbles (50, 51).

Field generation. US transducers utilize piezoelectric materials to generate traveling and standing sound fields (**Figure 3b**). These piezoelectric elements, ranging from 0.5 to 3 cm in dimension,

typically operate within a frequency range of 10 kHz to 10 MHz, generating pressure amplitudes on the order of kilopascals. Typically, low-frequency US waves can penetrate deeper into the body compared with high-frequency US waves. Lower-frequency US waves (0.5–3 MHz, used in therapeutic US) have longer wavelengths and can travel further into tissues, making them suitable for the active locomotion of microrobots within the body. The control and modulation of the electric field applied to the piezoelectric transducer are regulated by an electronic function generator, enabling the generation of US with specific frequencies and patterns.

US manipulation systems have gained significant attention for *in vivo* treatments. Recent advances have showcased the successful implementation of a HIFU transducer array to manipulate millimeter-sized glass spheres in a pig urinary bladder (52) and to trap and manipulate microbubbles in a mouse blood vessel within dorsal skin (53).

Challenges. Most locomotion experiments have been conducted in smaller animal models with vasculatures located on skin surfaces. There is a need to develop transducers capable of manipulating micron-sized objects at various depths within the living body.

Successful implementation of US-based microrobots in medical applications hinges on tackling numerous challenges. When deploying microrobots in *in vivo* conditions, it is crucial to consider specific US parameters, including attenuation and impedance mismatch. As US waves propagate through a biological medium, they experience attenuation or decay, gradually weakening the US signal as it travels deeper into the body. Furthermore, as US waves propagate through the body, they encounter various interfaces and compositions with different acoustic properties, as the living body is heterogeneous in material content. These interactions lead to partial transmission and reflection of the US energy at the interface. When US encounters bones with microstructural boundaries and pores, these interfaces and compositions cause the US waves to scatter in different directions. Thus, transmitting sound waves through the skull and bones becomes difficult, and predicting the sound field becomes challenging, making manipulation of US waves in these areas difficult or unpredictable. Understanding and accounting for these factors are essential for optimizing the performance and effectiveness of US-based microrobots in medical applications.

US directionality is another crucial aspect to consider. By incorporating microbubbles of different sizes in microrobot design, each with its unique resonance frequency, it becomes possible to steer the microrobot in a specific direction (42). However, steering considerations are necessary for nonresonant acoustic microrobots. In such cases, acoustic swimmers equipped with a phase transducer array could emerge as an excellent alternative for steering and propulsion.

Light

Light (electromagnetic radiation of wavelength 10–1,100 nm) can be used as an energy source for wireless actuation. Light is an extremely versatile energy source, as it can be tuned and optimized in terms of wavelength, energy, and polarization with high spatial and temporal resolution (54). Given these features, light has been proposed for untethered microrobot actuation. Here, we provide an overview of light-based actuation together with a description of actuation platforms and open challenges.

Overview and advantages. Light delivers an energy amount that is proportional to its frequency. At the same time, the delivered energy amount strongly depends on the properties of the propagation medium (materials, type of interfaces, optical properties) and on the optical features of the microrobot to be controlled. In this regard, most tissues are nontransparent to light, so absorption/scattering phenomena should be taken into account to prevent tissue damage and to ensure sufficient penetration depth. When the propagation medium is represented by biological

tissue, light penetration depth is significantly reduced due to absorption and scattering phenomena associated with chromophores and biological molecules.

Some regions of the electromagnetic spectrum, such as the near infrared (of wavelength 650–1,350 nm) offer the opportunity of higher penetration depth due to the lower light absorption associated with predominant molecules such as hemoglobin.

In optically driven microrobotics systems, the propulsion mechanism is typically based on the movement or deformation of body parts. Light can be used either as a direct actuation medium by inducing a state change in the actuator and task execution or by employing intermediate energy conversion methods to achieve actuation. Indeed, light can undergo transduction into heat (photothermal effect), conversion into electric fields (photoelectric effect), or catalysis of chemical reactions (photochemical effect) to induce changes in the constitutive microrobot materials. Direct light-based manipulation leverages the forces arising from focusing light with high-intensity gradients, as in optical tweezers (55). However, despite also allowing for 3D control, such methods suffer from extremely low output forces (in the piconewton range) and a limited compatibility within the *in vivo* environment (56).

In the majority of cases, light-responsive microrobots consist of polymers combined with metallic components to make them responsive to indirect light actuation mechanisms. Liquid-crystalline elastomers are abundantly used as artificial muscles to develop light-responsive microrobots due to their reversible large anisotropic deformation and relatively high output force upon triggering by photochemical reactions or photothermal heating (57, 58). Hydrogels whose polymeric chains are modified to endow them with light responsiveness are a valid alternative, as well. When focusing on these two classes of optical materials, their interaction with body tissues, as well as their capability of becoming biocompatible, buoyant, and suitable for 3D locomotion, prove favorable (59).

Light-responsive microrobots typically feature a speed of motion below a few body lengths per second due to the relatively slow response time of light-sensitive materials. They hold the advantage of high spatial selectivity in activation (thanks to laser-focusing opportunities) but at the cost of limited degrees of freedom unless complex 3D interference patterns are generated.

Light sources. Optical actuation can take place over an even larger distance, with laser beams capable of traveling in a straight line if they are not disturbed by interface media, such as biological tissues. Different types of light sources ranging from precise lasers—possibly with high power—to simple lamps can be employed to trigger light-responsive materials and structures. These types of stimulation equipment are in the several-centimeter scale, depending also on the output power, generation technology, and requirements in terms of precision and selectivity. Light distribution can be controlled both using laboratory-level devices, such as mirror scanners and digital micromirrors, and commercial digital strategies based on projectors to dynamically modulate the light pattern in geometry and wavelength at high frequencies (over 30 Hz) (**Figure 3c**).

Challenges. Challenges associated with light actuation lie in the need to find a proper compromise between safety, penetration depth, and the amount of transmitted light, to allow promotion of an effective actuation. Indeed, when targeting medical applications, light interaction with tissue should be considered both to prevent cellular damage and to allow sufficient penetration depth. Although some windows can be identified, light actuation generally fails to get deep into the body. One opportunity in this area is offered by using endoscopic and endovascular tools to bring light closer to the target working site by means of optical and laser fibers.

Additional challenges associated with light-triggered actuation lie in the relatively low response speed of light triggerable materials. Indeed, such materials require a significant structure

rearrangement, which significantly prolongs the response time, especially when submillimetric or millimetric structures are considered.

Hybrid Mechanisms

In traditional machines at the centimeter scale and above, mechanisms such as shafts, gears, and cables connected to dc motors allow for force transduction between translation and rotation, as well as force amplification. To scale down this approach, magnetic fields have begun to be used in synergy with miniature transmission mechanisms. Such mechanisms have been created for magnetic microrobots from the millimeter scale (60, 61) to the micrometer scale (62) and have been proposed to power end effectors such as microgrippers and cargo-release tools.

Millimeter-scale transmission mechanisms are being explored to increase the amount of force from externally driven magnetic mechanisms from the micronewton to the newton level. Microtransmission mechanisms based on traditional gearsets (63) have been proposed for this purpose. However, issues associated with friction must be taken into account. Nontraditional transmissions, for example, those based on a driving magnet and twisted string actuators (64), have promise but have yet to be applied at submillimeter scale. Such hybrid approaches have only begun to be explored, but there is still a great deal of potential to enhance the utility of any actuation method with such mechanisms.

MICROBOT TRACKING IN VIVO

Reaching specific targets within the body to perform medical tasks calls for fine control, which in turn requires information on microrobot position and activation state. Such closed-loop control is a traditional method in robotics, while the unique challenge for microrobotics is that most results accomplished so far in the field have been limited to the use of high-resolution optical microscopy in a laboratory environment. Optical microscopy gives excellent visualization but is a viable option only in highly superficial and transparent body areas, such as the eye. Tracking of tools for the entire medical robotics and smart devices field is an ongoing challenge, where inspiration on methods can come from what has been accomplished in these better-established fields (65).

Optical tracking represents the gold standard for pose estimation of medical tools outside the body, by employing a combination of markers mounted on the device and camera-based equipment for detection (66). However, in the absence of a direct line of sight, such methods fail (67). Sensor-based approaches such as electromagnetic tracking (68) can be used for tools out of the line of sight in the body. However, space constraints and requirements for untethered solutions limit the use of sensor-based tracking strategies in the medical microrobotics field. Image-based tracking stands out as a valid alternative to sensor-based strategies.

The introduction and use of images in the medical arena date back to 1895 with the invention of X-rays by the German physics professor Wilhelm Röntgen (69, 70). Since then, medical imaging has significantly advanced with a tremendous impact on diagnosis and medical robotics. When focusing on microrobotics, medical imaging methods will be critical to make the translation from a lab setting to the bedside possible. The specific imaging requirements depend on the features of each unique anatomical application area.

Medical imaging methods based on ultrasound, magnetic fields, light, ionizing radiation, or combinations of these have been proposed to track and monitor microrobots in tissues (71). In particular, US and magnetic field-based methods are being seen in the community as particularly versatile for microrobot tracking and are widespread both in clinics and in the microrobotics field (**Figure 4**).

US imaging

Magnetic imaging

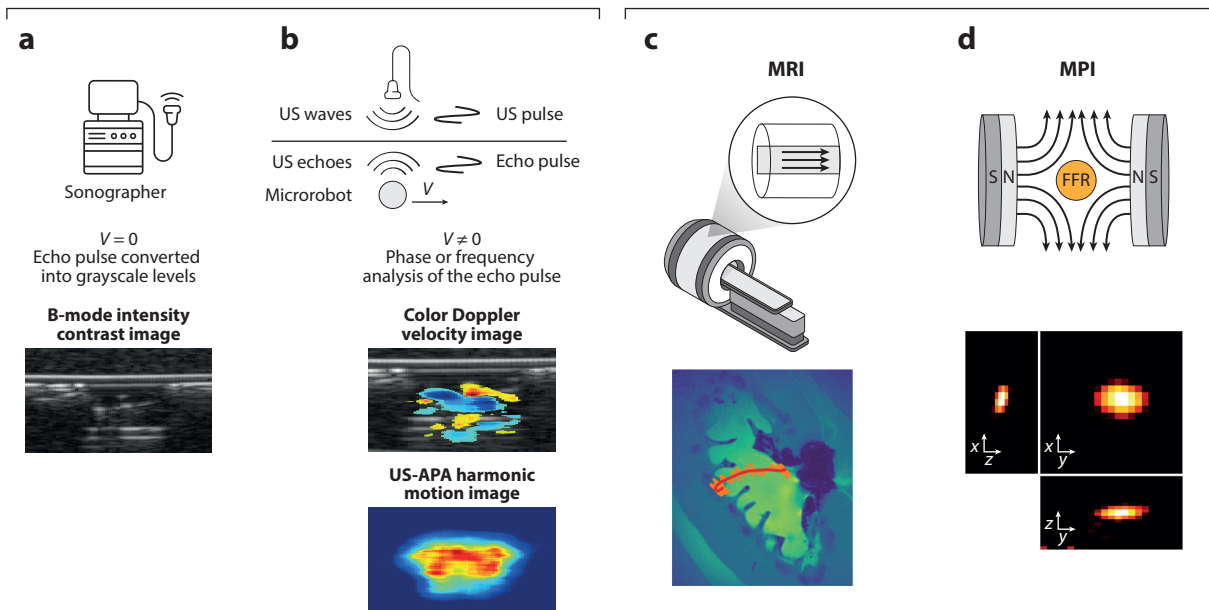


Figure 4

US and magnetic imaging in medical microrobotics. (a) Diagnostic US working principle: US waves emitted by the sonographer transducers are reflected back in the form of echoes. Intensity-based B-mode imaging is typically employed to visualize still objects (i.e., $V = 0$). (b) When the microrobot is moving, phase and frequency shift in the backscattered wave can be analyzed to enhance microrobot visualization, as in Doppler and US-APA imaging. Images of a helical magnetic microrobot are shown for the three methods. Images in panels *a* and *b* reproduced from Reference 72 (CC BY 4.0). (c) MRI exploits hydrogen atom excitation within a complex magnetic apparatus to provide structural tissue imaging and microrobot visualization. A paradigmatic example is shown of MRI-based microrobot tracking in ex vivo pig kidneys. Image in panel *c* reproduced from Reference 73 (CC BY 4.0). (d) MPI exploits magnetic material excitation and the shift of an FFR to provide the distribution of magnetic materials within a specific workspace. A paradigmatic example is shown of MPI-based microrobot tracking in a brain vasculature phantom. Image in panel *d* reproduced from Reference 74 (CC BY 4.0). Abbreviations: APA, acoustic phase analysis; FFR, field-free region; MPI, magnetic particle imaging; MRI, magnetic resonance imaging; US, ultrasound.

Selecting the imaging modality for a target biomedical application inherently requires a compromise between spatial and temporal resolution, penetration depth, safety, suitability for the target region, possibility to include dedicated contrast/imaging agents in the microrobot structure, and tracking precision.

Among all the aforementioned parameters, spatial and temporal resolution are of primary importance in selecting the most appropriate method. More specifically, spatial resolution can be defined as the minimal distance possible between two objects making them still distinguishable and should be comparable with microrobot size (body length) and features. This allows the assignment of physical dimensions to pixels and, thus, the derivation of target object dimensions and distances from the acquired images. Temporal resolution refers to the rate of data collection and ultimately indicates the amount of time needed for acquisition of each successive image.

Several imaging strategies have been employed to track microrobots. Given that the choice of the tracking method really depends on the target region, microrobot features, and tracking specifications, identifying a general-purpose optimal modality is not feasible. In fact, one trend in the state of the art is pursuing multimodal imaging and tracking strategies that combine the advantages of several imaging methods, where each method may be the most suitable for each

different phase of a procedure (e.g., preoperative planning, intraoperative tracking, and postoperative monitoring/verification). Some proposed strategies in this direction include multisource computed tomography (CT) imaging for intravascular interventions (75); combining CT, US, and MRI in chemoembolization procedures in pig liver (76); US and photoacoustic imaging in mice bladder (77); and CT combined with US for aneurysm filling (78).

With this awareness in mind, we analyze two main imaging strategies that stand out as particularly promising in different body regions.

Ultrasound-Based Imaging

US offers the opportunity of real-time imaging (at rates up to hundreds of frames per second) with no harm to tissues, using equipment that is low cost, compact, and portable (79). US interaction with tissues depends strongly on the pressure wave features (in particular, wave frequency) and on the number and type of tissues/interfaces to be crossed. Higher-frequency US waves experience higher attenuation in a medium due to increased wave interactions with the medium, resulting in lower penetration depth. On the other hand, higher US frequencies lead to higher image spatial resolution. High-frequency US waves (e.g., 12–15 MHz) allow for submillimeter resolution at small depths (3–4 cm), whereas low-frequency US waves (e.g., 3–5 MHz) achieve millimeter-scale resolution at high depth (20 cm).

There are multiple methods of processing ultrasound echo data into an image, with B-mode being the most common technique. As seen in **Figure 4a**, B-mode converts echo signal amplitude at each point in space into a brightness level to create an image. At first glance, a B-mode image looks like a picture of the anatomy, but echo amplitude depends multiply on US wave reflections, transmission, and attenuation upon interaction with tissues. Thus, B-mode images can contain many complex artifacts, rendering image interpretation a nuanced art. Image clarity depends significantly on the direction from which an image is taken, interface layers, and probe contact with the tissue, in addition to the properties of the target tissue/object.

Khalil et al. (80) demonstrated the feasibility of B-mode detection of *in vitro* micrometer-sized (100- μm) magnetic microrobots. In recent years, B-mode tracking has been integrated into robotic platforms, enabling closed-loop control of microrobots (81, 82), catheters (83), and millimeter-sized swarms of magnetic microparticles for blood clot removal (84). Contrast and pattern-matching techniques together with the definition of anatomy-based (e.g., within vessel boundaries) reduced regions of interest allow for microrobot detection and tracking in tissues. Because B-mode images can be complex to interpret, machine learning (ML) approaches using deep learning are recently being deployed, which use example images to allow automatic real-time microrobot detection (85, 86), tracking, and localization (87).

Despite the impressive speed and picture-like images created by the B-mode method, microrobots' low echogenicity can hamper their visualization and differentiation from highly complex soft tissues, especially when microrobots are moving close to a boundary (as in the case of microrobots moving in contact with vessel walls). To improve device contrast in B-mode images, ultrasound contrast agents such as air bubbles integrated on the device surface (88) can be exploited.

However, microrobot motion smaller than the US wavelength (in the 100–500- μm range for typical imaging frequencies) will not be detectable in B-mode imaging. To cope with this challenge, motion-based US imaging methods (**Figure 4b**) can play a role and outperform with respect to brightness-based B-mode imaging. These methods typically rely on the shift in frequency and phase of the acoustic wave when scattered back by a moving object. US Doppler-mode imaging uses such frequency-shift data to show the velocity of tissues/objects along with wave-propagation direction and is widely employed in clinical practice for vascular screening. Since the early 2000s, Doppler imaging has been used for tracking a catheter by detecting its vibrating tip (89, 90).

Doppler imaging has been successfully employed to localize both single microrobots (91) and swarms of microrobots (92, 93).

Recently, US acoustic phase analysis (US-APA) has been proposed to add selectivity to general-purpose Doppler imaging. Indeed, by analyzing the phase shift of the backscattered acoustic waves upon interaction with a moving object, information on the object displacement (even when the displacement is smaller than the wavelength of the US wave) can be detected by looking at this phase shift. US-APA relies on the processing of raw radiofrequency (RF) data through Fourier analysis and selective motion filtering, aimed at identifying specific motion features of the microrobots and at rejecting physiological motions not associated with microrobot movements. As compared with Doppler imaging, US-APA shows superior performance in complex, dynamic, and echogenic environments (72). US-APA proved robust with respect to different imaging conditions such as low-contrast or dynamic environments (e.g., microrobots, with dimensions ranging from 1,500 to 500 μm , in a phantom vessel with blood flow or tissue motion). Additionally, US-APA was also exploited for closed-loop control in a visual servoing platform (94). By relying on the analysis of raw RF data, it also shows a potential increase in spatial resolution [e.g., at 10 MHz, B-mode resolution is equal to 150 μm , while RF data can resolve up to 38 μm (95)]. However, a downside of US-APA is its low temporal resolution (a few frames per second) and its requirement of a precise knowledge of microrobot motion features (94–96).

Magnetic Field–Based Methods

Magnetic field-based imaging techniques rely on the application of an external magnetic field gradient to excite the atoms contained in the imaging target. They typically employ complex equipment including several electromagnets and associated powering and cooling apparatuses. Atom excitation is typically associated with a change in the magnetic moment and detected by receiving coils through induced flowing currents. Different excitation principles can be put in place to perform magnetic field-based imaging (97, 98). MRI is based on the nuclear magnetic imaging principle and refers to hydrogen atoms excitation (**Figure 4c**). As such, it is a structural imaging method, allowing at the same time retrieval of microrobot position and anatomical information. On the other hand, magnetic particle imaging (MPI) relies on the excitation of magnetic materials and does not allow the derivation of anatomical features.

MRI is widely employed in clinical practice. The technique features spatial resolutions as small as 500 μm of the voxel side but at the cost of long acquisition times—and, thus, reduced temporal resolution (up to minutes)—especially when 3D imaging is performed. Given that it is based on material and tissue composition, MRI can leverage the use of contrast agents based on iron oxide to enhance the detectability of certain anatomical structures or tools (e.g., microrobots).

The first studies also revealed one of the main advantages associated with MRI-based tracking, namely, the possibility of using the same apparatus for both actuation and tracking. While these two phases cannot be done simultaneously, time-sequenced alternation between imaging and tracking can make real-time tracking and closed-loop control possible (albeit at a slower speed).

Recent work proposed a 1D projection-based approach aimed at fast tracking of submillimetric ($\sim 300\text{-}\mu\text{m}$) microrobots. The method has been demonstrated both *in vitro* and *ex vivo* with tracking accuracies of several body lengths (73). Furthermore, the integration of deep learning strategies was investigated to enable 3D tracking from 2D MRI slices, thus enabling an increase in microrobot detection frequency (up to 1 Hz) (99). Interesting trends also focus on novel functionalization strategies aimed at enhancing MRI visualization of subresolution structures (100).

MPI provides an estimation of magnetic material distribution in the workspace by exploiting the superposition of time-varying and static magnetic fields to create a field-free region within the workspace whose position determines the magnetic materials' response to excitation fields and the

possibility of mapping their distribution (**Figure 4d**). Similar to MRI, MPI scanners have been employed at the same time for tracking and navigation control (101). At present, MPI features resolutions of 1 mm to a few millimeters and temporal resolution strongly related to the workspace dimension. For example, the commercial Bruker preclinical MPI scanner features a speed of 46 volumes/s (102). Furthermore, typical MPI equipment features small workspaces or performance deterioration when the workspace is scaled up (103).

MPI has a demonstrated ability to use magnetic fields for various purposes such as nanoparticle tracking and control. Moreover, the high temporal resolution makes it suitable for real-time control. On the other hand, the poor spatial resolution of MPI hampers the tracking of micrometer-scale devices. One recent work successfully used MPI to control navigation and to track a 3-mm helical microrobot in a vascular phantom for aneurism treatment. This method had a tracking error of approximately 0.25 body lengths (74).

MICROBOTS FOR BIOMEDICINE

Microrobots have been proposed extensively for performing medical tasks ranging from minimally invasive surgery to targeted drug delivery and health monitoring. As overviewed in the previous sections, energy delivery, actuation, and tracking strategies allowing untethered locomotion and task activation for microrobot-based therapy in clinical practice have been investigated. Given their noninvasive dexterity, microrobots hold the promise to overcome biological barriers and technological bottlenecks seen with traditional interventional tools and therapeutical strategies. Targeted drug delivery stands out as a relatively simple task (in particular due to the low precision needed and the reduced force output requirements) and, thus, represents the most-investigated, near-term, and promising application scenario for microrobots. In this area, microrobots can produce significant advancements over the low efficiency of nanomedicine-based and traditional drug administration strategies (104). In the following sections, the main results accomplished when using microrobots as tools to perform medical tasks in the circulatory system, the GI tract, and other relevant body regions are reviewed.

Microrobots for the Vascular System

Miniaturized robots navigating within the vasculature under physiological flow conditions show great potential for treating a number of diseases. In particular, microrobots have the potential to revolutionize traditional systemic therapies through precision-focused methods that administer treatments to particular lesions, enhancing intervention effectiveness for ailments including but not limited to stroke, peripheral artery disease, abdominal aortic aneurysm, carotid artery disease, pulmonary embolism, atherosclerosis, and cancer.

Our 3D vascular networks include large arteries with high flow velocities and pulsatile flow, and microrobots must demonstrate the ability to propel themselves under such conditions and navigate the intricate vasculature. Previous research has primarily focused on controlling microrobot trajectories within microchannels and confined spaces, with most studies attempting manipulation under static conditions (52, 105, 106). Recent investigations have explored microrobot capabilities under externally controlled flow conditions, showing that navigation tends to be impeded as flow rate increases (107). This limitation arises from the drag force, when encountering physiological flow rates up to several centimeters per second. As a result, most engineered microrobots cannot withstand the drag force and are swept away. Addressing the challenge posed by physiological flow is crucial to unlock the full potential of microrobots for medical applications.

To enable propulsion against flow, researchers have drawn inspiration from the intelligent techniques observed in natural swimmers and have taken advantage of boundary conditions (108,

109). In a purely physical approach, biomimetic colloidal particles can get near a boundary, such as a vessel wall, and move upstream under acoustic or magnetic fields, either singly or in combination. For instance, one recent work (**Figure 5a**) achieved upstream motion along a vessel with acoustomagnetically activated, self-assembling microrobots (110, 111). Other works demonstrated upstream manipulation of magnetically guided Janus particles, effectively utilizing their antibody-mediated targeting capabilities to deliver drugs selectively into specific tumor sites (107). Upstream navigation of magnetic microrollers on diverse 3D surface topographies that mimic biological microtopographies are shown in **Figure 5b** (112).

However, despite the promise of these studies, there remain challenges to be addressed such as slow propulsion velocities and precise control against physiological flow rates. Recently, showcases of upstream and cross-stream propulsion of ultrasonically activated self-assembled microbubbles have been made within a physiological environment and against a flow rate of 16.7 cm/s (50, 113) (**Figure 5c**).

To achieve successful deployment of microrobots in the vasculature, the devices must be constructed from materials and structures that can withstand the cyclic stresses induced by pulsatile flow and operate reliably without structural failures. Furthermore, the microrobots must be designed to avoid damaging the vessels' endothelium during navigation. Additionally, the propulsion system should be able to adapt to varying conditions; in particular, changes in flow velocity and direction during different phases of the cardiac cycle may affect microrobot propulsion and maneuverability. The presence of vascular diseases such as atherosclerosis and aneurysms, which are known to alter flow characteristics and cause disturbed flow patterns, presents further challenges to the effective operation of vascular microrobots.

In addition to manipulating microrobots, there is a surging interest in manipulating microcatheters within the vascular network, which can grant access to intricate and hard-to-reach anatomical regions within the body. In particular, 3D-manipulated microcatheters have emerged as innovative tools in medical applications, offering precise, flexible, and accurate navigation capabilities for minimally invasive therapeutic procedures, while overcoming the bottlenecks of wireless tools design. Current approaches to steering and manipulating microcatheters in 3D environments have primarily utilized magnetic fields. In one study, a mechanism for flow-driven advancement and magnetic steering of flexible microcatheters was shown first in bifurcated channels, and then its efficacy was validated within *ex vivo* rabbit ears (114). In another study, a magnetic microcatheter that employed a cylindrical bar magnet connected to a robotic arm for precise maneuvering achieved real-time 3D navigation in conjunction with X-ray fluoroscopy. This system was able to effectively navigate complex pathways in both *in vitro* tests using neurovascular phantoms and *in vivo* evaluations in a porcine brachial artery (115), as shown in **Figure 5d**. Researchers are continuously exploring innovative strategies for the development of microcatheters. A multifunctional microcatheter made by rolling flexible polymeric films containing integrated electronics is intended to provide drug delivery, micromanipulation, tracking, and navigation capabilities with feedback-driven control using a magnetic sensor (116), as shown in **Figure 5e**. A submillimeter-diameter endovascular microcatheter was made steerable by incorporating soft-bodied hydraulic actuators at the distal tip. The capability of this microcatheter to navigate through vessels and implant embolization coils in cerebral vessels was demonstrated in a live porcine model (117), as shown in **Figure 5f**. One design integrated three metallic wires into a microfiber, enabling precise control of the fiber's movement in 3D space by adjusting the length of each wire (118).

Microrobots and microcatheters used in biomedicine must be designed to interact precisely with cells and biomolecules while minimizing adverse effects. Biocompatible coatings and surface modifications are necessary to optimize microrobot surface properties to help reduce unwanted

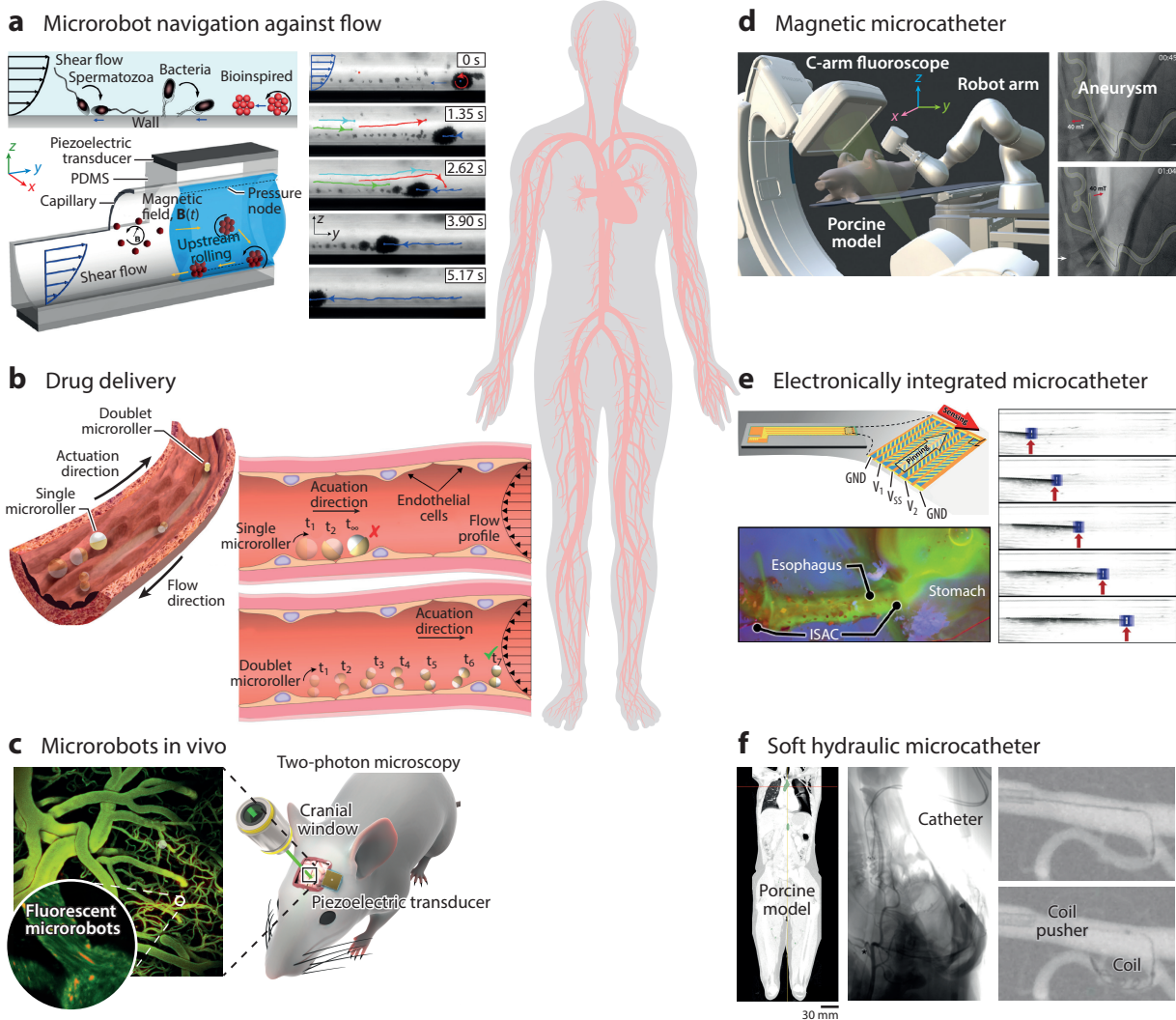


Figure 5

Microrobots and microcatheters for use in the vascular system. (a) Biological microswimmers, such as spermatozoa and bacteria, skillfully leverage no-slip boundary conditions to move upstream along walls. Drawing inspiration from this natural phenomenon, researchers developed acoustomagnetic microrobots that first self-assemble in a rotating magnetic field, then upon application of an acoustic field swiftly move toward the wall and then upstream (111). (b) Magnetic single and doublet Janus particles demonstrate navigation and upstream manipulation capabilities on diverse 3D surface topographies. Panel adapted from Reference 112 (CC BY 4.0). (c) Manipulation of acoustically activated self-assembled microrobots in the mouse brain vasculature. Panel adapted from Reference 113 (CC BY 4.0). (d) The experimental setup of a magnetic microcatheter, which includes a cylindrical magnet connected to a robotic arm for precise manipulation and real-time 3D X-ray fluoroscopy for guidance. The image sequence demonstrates the navigation of the microcatheter in a brain aneurysm. Panel adapted with permission from Reference 115. (e) A multifunctional microcatheter was developed by rolling flexible polymeric films containing integrated electronics, aimed at providing drug delivery, micromanipulation, tracking, and navigation capabilities with feedback-driven control using a magnetic sensor. Panel adapted from Reference 116 (CC BY 4.0). (f) A soft-bodied hydraulic actuator is incorporated at the distal tip of an endovascular microcatheter. Panel adapted with permission from Reference 117. Abbreviations: GND, ground; ISAC, immune-stimulating antibody conjugate; PDMS, polydimethylsiloxane; SS, source supply; V, voltage.

interactions with blood components, lowering the risk of immune adverse reactions, clotting, and inflammation.

Microrobots for the Gastrointestinal Tract

The GI system contains difficult-to-reach segments and includes barriers (e.g., in terms of drug absorption) that motivate the development of microrobots intended for the GI tract. Given the discomfort and pain associated with traditional endoscopic procedures, endoscopic capsule robots were proposed more than 20 years ago as untethered tools to perform diagnostic examinations in the GI tract (119). While endoscopic capsule robots are not in the scope of this review, capsule robots, as well as instrumented endoscopes, have the tremendous merit of having provided a wide awareness and a wide set of specifications on how microrobots for operation in tubular organs should be designed.

The GI system features a low immune response compared with the vascular system, but physical (mucus layer) and chemical (absorption across the mucosa) barriers make targeted drug delivery, biopsy, and other interventional tasks challenging without highly controllable small-scale devices.

The complexity of the GI system in terms of its path-winding nature, the presence of villi and mucus, and the distance from the body surface (where external control field sources could be placed) make locomotion and target reaching in specific segments of this region challenging. Recent efforts have been directed toward strategies for enhanced magnetic locomotion across the GI tract.

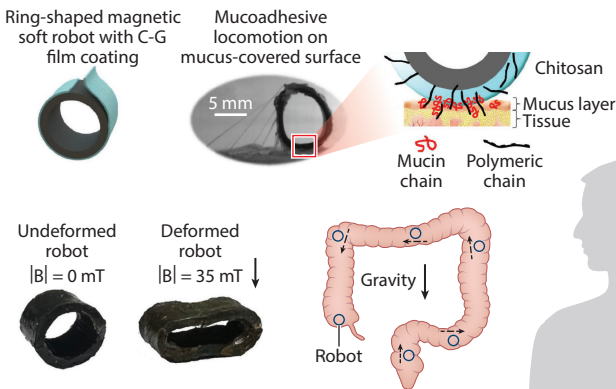
Film-like, magnetic, soft microrobots capable of multimodal locomotion have been proposed and optimized to cope with navigation in this challenging environment. A porous, silica-doped, soft magnetic microrobot was proposed for improving locomotion across nonideal environments in the presence of peristalsis-like disturbances. Optimized adhesion properties and higher mechanical stability were pursued to this aim (120). Mucoadhesive coatings (121) (**Figure 6a**) and peeling-and-loading microneedle-based mechanisms (122) have been implemented on board film-like, magnetic, soft milliscale robots to enhance the robots' capability to climb and move along complex, wet surfaces, as well as along ex vivo porcine intestine tissue.

Given the size of the GI system, both milliscale robots and swarms of micrometer-scale robots have been proposed for a variety of applications including targeted drug delivery, gastric bleeding treatment, biopsy, sensing, and physical therapy (i.e., mediated by electrical and thermal stimulation).

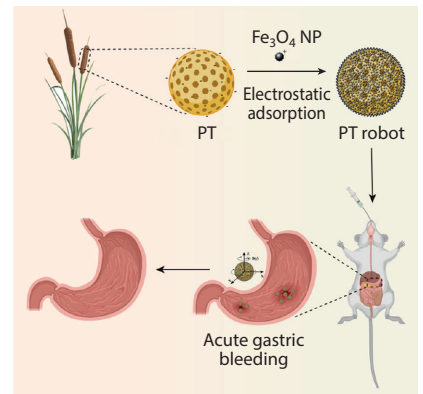
The motivation to perform targeted drug delivery in the GI system arises from the rapid degradation of biomacromolecules and poor absorption in the GI tract, which limits the efficacy of oral administration of several classes of drugs. Developing oral delivery systems that are able to reach specific locations and allow for efficient drug absorption across the GI mucosa is an opportunity for which microrobotics solutions are being proposed. Inspired by the leopard tortoise's ability to passively reorient, researchers have developed a self-orienting millimeter-scale robot that is able to magnetically reach a target location and deploy drug-loaded microneedles for gastric macromolecules delivery across the mucosa (123). Other interesting works combine an anchoring mechanism and a drug-release system activated synchronously by a rotating magnetic field to withstand peristalsis while ensuring targeted delivery of therapeutics (124). Microrobot swarms based on magnetized pollen typhae (20 μm each) proved efficient in stimulating endogenous blood coagulation pathways to treat gastric bleeding in living mice (125) (**Figure 6b**).

Recently, quadruped, soft, thin-film microrobots able to achieve multiple controllable locomotion modes under oscillating magnetic fields proved efficient in pick-and-place tasks in complex

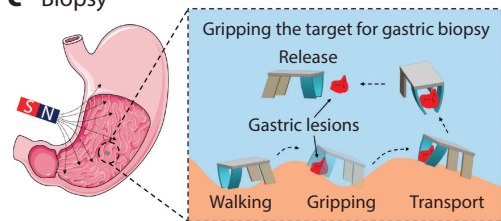
a Strategies for enhanced locomotion



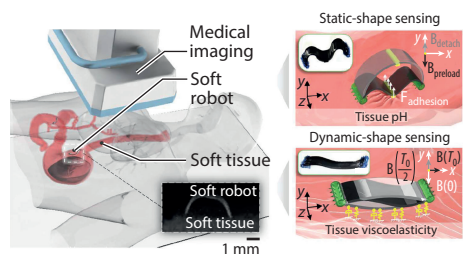
b Drug delivery



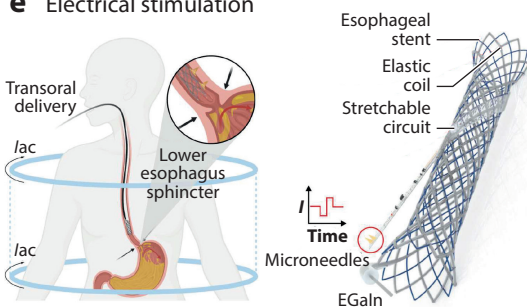
c Biopsy



d Sensing



e Electrical stimulation



f Hyperthermia

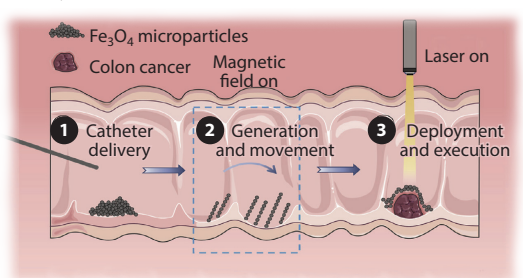


Figure 6

Microrobots in the GI system. The complexity of the GI system in terms of its path-winding nature, the presence of villi and mucus, and the distance from the body surface make locomotion and target reaching in specific segments of this region challenging. To cope with this challenge while performing medical tasks, several approaches have been proposed, and paradigmatic examples are shown here. (a) Strategies for enhanced locomotion based on a mucoadhesive coating placed over magnetic soft microrobots. Panel adapted from Reference 121 (CC BY 4.0). (b) Magnetized PT-based microrobot swarm for gastric bleeding treatment. Panel adapted with permission from Reference 125. (c) A quadruped, soft, thin-film microbot able to achieve multiple controllable locomotion modes and eligible for biopsy in the GI system. Panel adapted from Reference 126 (CC BY 4.0). (d) Magnetic field-based tissue properties sensor for GI tract diagnostic investigations. Panel adapted from Reference 127 (CC BY 4.0). (e) A battery-free and deformable electronic esophageal stent for lower esophageal sphincter stimulation through electromagnetic coupling. Panel adapted from Reference 128 (CC BY 4.0). (f) A magnetic microbot swarm for flexible deployment and laser-mediated photothermal therapy. Panel adapted with permission from Reference 130 (CC BY 4.0). Abbreviations: EGaIn, eutectic gallium-indium; GI, gastrointestinal; NP, nanoparticle; PT, pollen typhae.

stomach-like environments, paving the way to magnetic microrobot-based biopsy in the GI system (126), as seen in **Figure 6c**.

Magnetic soft microrobots have also been proposed for performing diagnostic tasks by exploiting their change in magnetic response. By controlling robot–tissue interaction using external magnetic fields, visualized by medical X-ray or US imaging, tissue properties can be derived precisely from the robot shape and magnetic fields (127), as seen in **Figure 6d**.

Wireless energy transfer to microrobots operating in the GI system can serve to activate locomotion and drug delivery, as in the aforementioned cases. However, additional energy transduction mechanisms can occur on board, to perform both electrical stimulation and hyperthermia. A battery-free and deformable electronic esophageal stent was proposed for noninvasive wireless stimulation of the lower esophageal sphincter. The compliant stent consists of an elastic receiver antenna filled with liquid metal. Electromagnetic coupling with an external antenna allows current flow across the stent and sphincter stimulation through dedicated anchoring needles (128), seen in **Figure 6e**. Metallic structures on board film-based milliscale robots and microrobot swarms were employed for tissue hyperthermia. In the first case, a pangolin-inspired, bilayered soft robot was proposed. When triggered with RF fields, heating greater than 70°C at large distances over 5 cm within a short period of time (less than 30 s) could be achieved by exploiting both Joule heating and hysteresis losses (129). A microrobot swarming strategy was proposed to organize microscale magnetic microrobots into millimeter-height cilia-like structures, endowing the microrobot swarms with more powerful capabilities to pass obstacles and achieve flexible deployment, as well as laser-mediated photothermal therapy (130), as seen in **Figure 6f**.

Microrobots in Other Regions

In light of their potential dexterity and capability to execute precise tasks, microrobots have also been proposed for operation in regions beyond the vasculature and GI tract, where additional functionalities, such as delivery of cells or embryos, have been demonstrated.

Brain. In the brain, microrobots are being explored for targeted drug and cell delivery through the vasculature or within the cerebral spinal fluid at the micrometer scale. Future treatments such as stem cell therapy would require placement of cells in precise areas of damaged tissue, which can be done noninvasively with targeted precision using microrobots (131). Brain tissue is significantly softer than other tissues in the body, thus representing an opportunity for microrobots, which may not be able to exert sufficient forces to manipulate or cut other tissues. Endoscopic approaches to neurosurgery are not used commonly due in part to the size and dexterity of available tools. Remotely powered and controlled robots at the millimeter scale are being explored for minimally invasive neurosurgery using magnetic actuation (132), with the potential to scale to hundreds-of-micrometer sizes. One challenge in the brain is that US does not penetrate through the skull easily, so other imaging solutions such as endoscopic cameras for surgery or fluoroscopy for wireless guidance would be required.

Eye. Developing microrobots for operating in the eye has been a priority since the beginning of medical microrobotics (133), and microrobots have been reported both for microsurgical and drug delivery tasks. A swarm of helical submicrometer propellers featuring a liquid coating to minimize adhesion on a vitreous biopolymeric network was proposed for intravitreal delivery of therapeutic agents. Clinical optical coherence tomography and magnetic actuation were used to monitor and control the movement of the propellers and confirm their arrival on the retina near the optic disk (3). Recently, an untethered, shape memory alloy-based, 65- μm -long microrobot responsive to laser-induced propulsion through optothermal and optical trapping effects

was proposed for intraocular surgery (134). Magnetic navigation was also employed to perform intraocular injections through a flexible magnetic microcannula. Remarkably, real-time tracking and semiautomatic placement of the cannula were demonstrated toward the definition of more standardized microrobot-based interventional procedures (135).

Lungs. The narrow airways of the bronchial tubes and lungs are difficult to access for nonsurgical diagnosis of lung cancer by nodule biopsy. Flexible bronchoscopes can bend to navigate the larger first stages of bronchial tubes under fluoroscopic guidance, but to access the deepest locations within the lungs a smaller flexible instrument or an untethered solution is required. The commercial Monarch™ (Johnson & Johnson) and Ion (Intuitive Surgical) bronchoscopy robots are smaller in size at 3.5–4.2 mm, but an even smaller size is required for this procedure. Magnetically guided microrobotic catheters of approximately 2 mm in width can fully conform to the airway anatomy and access the majority of the airways (136).

Bladder. The bladder can be accessed readily by catheterization, with potential microrobotics treatments for ailments such as kidney stone breakup using a steerable microrobot within the kidney (137). Swarms of microrobots have been shown to move on ex vivo bladder tissue (138). Robotic devices at the centimeter scale have been shown to be able to help control bladder voiding (139).

Reproductive tract. Infertility affects tens of millions of couples, with many treatments such as in vitro fertilization and intracytoplasmic sperm injection requiring the egg to be fertilized outside the body before being reimplanted in the uterus. Microrobots are being explored for reproductive assistance directly in the female reproductive tract. Microrobots carrying sperm cells are being explored to guide fertilization directly to the egg within the uterus to address low sperm mobility (140) and for embryo implantation within the fallopian tube after in vitro fertilization (141). Under US guidance, swimming microrobots can be navigated after injection into the uterus and have been shown to function in microfluidic environments.

OPEN CHALLENGES AND CONCLUSIONS

In this review, we summarize medical and technical principles intended to guide the next generation of medical microrobotics experts in the design of novel miniaturized therapeutic tools. In doing so, recent relevant advancements, both from a technological and application-oriented perspective, are presented for different classes of medical microrobots. The application area determines several microrobots features, such as size, mechanical properties, force output, functionalization, and composition, but also the choice of the actuation and tracking strategies to be put in place for controlled target reaching and task execution.

The past few years have witnessed tremendous advancements in the field of medical microrobotics with the first in vivo demonstrations in large animals. These works represent a milestone by demonstrating that microrobots performing medical tasks in the body can become a reality and go beyond science fiction. Despite encouraging advancements and potentialities, we can still identify a set of issues and challenges that must be faced to pave the way of medical microrobots to the bedside.

Microrobots need to be better engineered to cope with biological barriers and ensure their safety. The choice of the constitutive materials is crucial in this context. Eligible materials must be biocompatible and/or biodegradable, cause no immune system response, and be functional (i.e., allowing for drug loading and optimized response to external control fields). The long-term fate of microrobots and their constitutive components should be assessed while looking for either full degradability (142), long-term residence in the body as in the case of implants, or strategies to

retrieve them upon task execution. Devising suitable retrieval strategies also copes with the need to address potential microrobot failures during task execution. In this regard, a proper compromise between degradation, component lifetime/clearance, and retrieval should be devised to guarantee that safety, yet not increasing invasiveness, is put into place for failure handling (143). Furthermore, open avenues to be investigated deal with sterilization and biological assessment toward future regulatory approval.

The structure of microrobots should also be further engineered to better support their functionality. Recent works have unveiled the possibility of using microrobots as smart responsive stents, tools for optimized embolization, and surgical tools. Developing new strategies for exerting higher forces with microrobotics tools is now required to go beyond simple targeted drug delivery.

In addition to a more efficient and biocompatible structure, microrobots need better control. This applies particularly to less-mature technologies such those based on US. The field of US-controlled robotics is a relatively new area; as a result, control and automation using this feedback modality are not yet well developed in comparison with magnetic and other robotic systems. The practical application of US-controlled microrobots is currently limited by the lack of robust automation and control systems. To fully integrate US technology into medical settings, it is crucial to invest in the development of advanced control strategies allowing manipulation and navigation in 3D spaces within the living body. The development of novel control strategies is strictly bound to the inclusion of real-time high-resolution tracking strategies (144) in the control loop toward closed-loop control and task automation.

A primary challenge for implementing meaningful ML solutions to microrobotics problems is now in generating realistic large datasets, so efforts to publish and describe such datasets will be instrumental (145). Published datasets for common experimental platforms have allowed ML solutions to advance at an astonishing rate in other fields, and the microrobotics community should consider where common platforms could be used widely to benefit similarly. A major development and employment of open platforms (e.g., the Robot Operating System for robotics, GitHub for software and data sharing, and using imaging equipment that allows access to raw data) will be crucial in this regard. Other robotic communities, such as researchers in continuum robotics, are moving in this direction with highly successful results (<https://www.opencontinuumrobotics.com/>).

Moving to the next steps in terms of technological and applicational maturity toward clinical use also calls for testing and performance evaluation benchmarks (e.g., in areas of tracking/control accuracy assessment and magnetic field generation system characterization). Open platforms could be used to benchmark feedback or control approaches.

Last but not least, a larger involvement of medical doctors in the microrobot design and evaluation process will be crucial in the future. At the same time, training of clinicians will be a key step to make them interested in and fully able to utilize microrobotics tools. Such training will help in pushing the current technological boundaries (e.g., those associated with medical imaging methods employment) and in supporting clinicians' awareness and acceptance/adoption of new technologies. Indeed, some lessons can be learned from robotic surgery and telemedicine, where clinician training is part of the design and assessment process for novel devices and helps support new technology adoption in clinical practice (146).

A joint interdisciplinary effort will be fundamental for moving microrobots to the bedside and producing a clinical impact in some selected applications. Preliminary *in vivo* validations have proved that there is room for bringing microrobots to the clinic—we should together exploit this positive moment to identify procedures in which microrobots can play a pivotal role and make a societal and healthcare impact.

DISCLOSURE STATEMENT

The authors are not aware of any affiliations, memberships, funding, or financial holdings that might be perceived as affecting the objectivity of this review.

ACKNOWLEDGMENTS

VI. and A.M. acknowledge the support provided by the European Union's Horizon Europe research and innovation program under grant agreement 101070066 (REGO). D.A. gratefully acknowledges the support provided by the European Research Council, as part of the European Union's Horizon 2020 research and innovation program (grant agreement 853309, SONOBOTS). D.A. also extends thanks to Zhiyuan Zhang, Alexia Del Campo Fonseca, and Prajwal Agrawal for helpful discussions.

LITERATURE CITED

1. Abbott JJ, Nagy Z, Beyeler F, Nelson BJ. 2007. Robotics in the small, part I: microbotics. *IEEE Robot. Autom. Mag.* 14(2):92–103
2. Nelson BJ, Kaliakatsos IK, Abbott JJ. 2010. Microrobots for minimally invasive medicine. *Annu. Rev. Biomed. Eng.* 12:55–85
3. Wu Z, Troll J, Jeong H-H, Wei Q, Stang M, et al. 2023. A swarm of slippery micropropellers penetrates the vitreous body of the eye. *Sci. Adv.* 4(11):eaat4388
4. Gwisai T, Mirkhani N, Christiansen MG, Nguyen TT, Ling V, Schuerle S. 2023. Magnetic torque-driven living microrobots for increased tumor infiltration. *Sci. Robot.* 7(71):eabo0665
5. Barducci L, Norton JC, Sarker S, Mohammed S, Jones R, et al. 2020. Fundamentals of the gut for capsule engineers. *Prog. Biomed. Eng.* 2(4):42002
6. Cheng LK. 2015. Slow wave conduction patterns in the stomach: from Waller's foundations to current challenges. *Acta Physiol.* 213(2):384–93
7. Miftahof RN. 2005. The wave phenomena in smooth muscle syncytia. *In Silico Biol.* 5:479–98
8. Woods SP, Constandinou TG. 2013. Wireless capsule endoscope for targeted drug delivery: mechanics and design considerations. *IEEE Trans. Biomed. Eng.* 60(4):945–53
9. Shenoy SS, Lui F. 2022. *Neuroanatomy, Ventricular System*. Treasure Island, FL: StatPearls Publ.
10. Purdy PD, Fujimoto T, Replogle RE, Giles BP, Fujimoto H, Miller SL. 2005. Percutaneous intraspinal navigation for access to the subarachnoid space: use of another natural conduit for neurosurgical procedures. *Neurosurg. Focus* 19(1):E11
11. Stan RV. 2007. Endothelial stomatal and fenestral diaphragms in normal vessels and angiogenesis. *J. Cell. Mol. Med.* 11(4):621–43
12. Duffner F, Schiffbauer H, Glemser D, Skalej M, Freudenstein D. 2003. Anatomy of the cerebral ventricular system for endoscopic neurosurgery: a magnetic resonance study. *Acta Neurochir.* 145(5):359–68
13. Ullrich F, Bergeles C, Pokki J, Ergeneman O, Erni S, et al. 2013. Mobility experiments with microrobots for minimally invasive intraocular surgery. *Investig. Ophthalmol. Vis. Sci.* 54(4):2853–63
14. Risquez F, Confino E. 1993. Transcervical tubal cannulation, past, present, and future. *Fertil. Steril.* 60(2):211–26
15. Nauber R, Goudu SR, Goeckenjan M, Bornhäuser M, Ribeiro C, Medina-Sánchez M. 2023. Medical microrobots in reproductive medicine from the bench to the clinic. *Nat. Commun.* 14(1):728
16. Eisentraut M, Sabri A, Kress H. 2023. The spatial resolution limit of phagocytosis. *Biophys. J.* 122(5):868–79
17. Yasa IC, Ceylan H, Bozuyuk U, Wild A-M, Sitti M. 2020. Elucidating the interaction dynamics between microswimmer body and immune system for medical microrobots. *Sci. Robot.* 5(43):eaaz3867
18. Champion JA, Walker A, Mitragotri S. 2008. Role of particle size in phagocytosis of polymeric microspheres. *Pharm. Res.* 25(8):1815–21

19. Gustafson HH, Holt-Casper D, Grainger DW, Ghandehari H. 2015. Nanoparticle uptake: the phagocyte problem. *Nano Today* 10(4):487–510
20. Greish K. 2010. Enhanced permeability and retention (EPR) effect for anticancer nanomedicine drug targeting. In *Cancer Nanotechnology: Methods and Protocols*, ed. SR Grobmyer, BM Moudgil, pp. 25–37. Totowa, NJ: Humana Press
21. Rogers DF. 2004. Airway mucus hypersecretion in asthma: an undervalued pathology? *Curr. Opin. Pharmacol.* 4(3):241–50
22. Meyerholz DK, Stoltz DA, Pezzulo AA, Welsh MJ. 2010. Pathology of gastrointestinal organs in a porcine model of cystic fibrosis. *Am. J. Patbol.* 176(3):1377–89
23. Fang J, Wang H, Xue Z, Cheng Y, Zhang X. 2021. PPAR γ : the central mucus barrier coordinator in ulcerative colitis. *Inflamm. Bowel Dis.* 27(5):732–41
24. Wong A, Ye M, Levy A, Rothstein J, Bergles D, Searson P. 2013. The blood-brain barrier: an engineering perspective. *Front. Neuroeng.* 6:7
25. Konofagou EE, Tunga Y-S, Choia J, Deffieux T, Baseria B, Vlachosa F. 2012. Ultrasound-induced blood-brain barrier opening. *Curr. Pharm. Biotechnol.* 13(7):1332–45
26. Saraiva C, Praça C, Ferreira R, Santos T, Ferreira L, Bernardino L. 2016. Nanoparticle-mediated brain drug delivery: overcoming blood-brain barrier to treat neurodegenerative diseases. *J. Control. Release* 235:34–47
27. Ballestín A, Malzone G, Menichini G, Lucattelli E, Innocenti M. 2022. New robotic system with wristed microinstruments allows precise reconstructive microsurgery: preclinical study. *Ann. Surg. Oncol.* 29(12):7859–67
28. Cianchetti M, Ranzani T, Gerboni G, Nanayakkara T, Althoefer K, et al. 2014. Soft robotics technologies to address shortcomings in today's minimally invasive surgery: the STIFF-FLOP approach. *Soft Robot.* 1(2):122–31
29. Abbott JJ, Diller E, Petruska AJ. 2020. Magnetic methods in robotics. *Annu. Rev. Control Robot. Auton. Syst.* 3:57–90
30. Wang B, Chan KF, Yuan K, Wang Q, Xia X, et al. 2022. Endoscopy-assisted magnetic navigation of biohybrid soft microrobots with rapid endoluminal delivery and imaging. *Sci. Robot.* 6(52):eabd2813
31. Yu J, Jin D, Chan KF, Wang Q, Yuan K, Zhang L. 2019. Active generation and magnetic actuation of microrobotic swarms in bio-fluids. *Nat. Commun.* 10(1):5631
32. Ishiyama K, Arai KI, Sendoh M, Yamazaki A. 2000. Spiral-type micro-machine for medical applications. In *Proceedings of 2000 International Symposium on Micromechatronics and Human Science (MHS2000), Nagoya, Japan*, pp. 65–69. New York: IEEE
33. Petruska AJ, Nelson BJ. 2015. Minimum bounds on the number of electromagnets required for remote magnetic manipulation. *IEEE Trans. Robot.* 31(3):714–22
34. Yang L, Zhang M, Yang Z, Yang H, Zhang L. 2022. Mobile ultrasound tracking and magnetic control for long-distance endovascular navigation of untethered miniature robots against pulsatile flow. *Adv. Intell. Syst.* 4(3):2100144
35. Heunis CM, Silva B, Sereni G, Lam MCW, Belakhal B, et al. 2023. The flux one magnetic navigation system: a preliminary assessment for stent implantation. *IEEE Robot. Autom. Lett.* 8(9):5640–47
36. Ryan P, Diller E. 2017. Magnetic actuation for full dexterity microrobotic control using rotating permanent magnets. *IEEE Trans. Robot.* 33(6):1398–409
37. Mahoney AW, Abbott JJ. 2015. Five-degree-of-freedom manipulation of an untethered magnetic device in fluid using a single permanent magnet with application in stomach capsule endoscopy. *Int. J. Robot. Res.* 35(1–3):129–47
38. Pittiglio G, Brockdorff M, da Veiga T, Davy J, Chandler JH, Valdastrì P. 2023. Collaborative magnetic manipulation via two robotically actuated permanent magnets. *IEEE Trans. Robot.* 39(2):1407–18
39. Carpi F, Pappone C. 2009. Stereotaxis Niobe[®] magnetic navigation system for endocardial catheter ablation and gastrointestinal capsule endoscopy. *Expert Rev. Med. Devices* 6(5):487–98
40. Petruska AJ, Edelman J, Nelson BJ. 2017. Model-based calibration for magnetic manipulation. *IEEE Trans. Magn.* 53(7):1–6
41. Xiang Y, Zhang J. 2023. A theoretical investigation of the ability of magnetic miniature robots to exert forces and torques for biomedical functionalities. *IEEE Robot. Autom. Lett.* 8(3):1771–77

42. Ahmed D, Lu M, Nourhani A, Lammert PE, Stratton Z, et al. 2015. Selectively manipulable acoustic-powered microswimmers. *Sci. Rep.* 5(1):9744
43. Ren L, Nama N, McNeill JM, Soto F, Yan Z, et al. 2023. 3D steerable, acoustically powered microswimmers for single-particle manipulation. *Sci. Adv.* 5(10):eaax3084
44. Wang W, Castro LA, Hoyos M, Mallouk TE. 2012. Autonomous motion of metallic microrods propelled by ultrasound. *ACS Nano* 6(7):6122–32
45. Ahmed D, Baasch T, Jang B, Pane S, Dual J, Nelson BJ. 2016. Artificial swimmers propelled by acoustically activated flagella. *Nano Lett.* 16(8):4968–74
46. Bertin N, Spelman TA, Stephan O, Gredy L, Bourriau M, et al. 2015. Propulsion of bubble-based acoustic microswimmers. *Phys. Rev. Appl.* 4(6):64012
47. Aghakhani A, Yasa O, Wrede P, Sitti M. 2020. Acoustically powered surface-slipping mobile microrobots. *PNAS* 117(7):3469–77
48. Ahmed D, Dillinger C, Hong A, Nelson BJ. 2017. Artificial acousto-magnetic soft microswimmers. *Adv. Mater. Technol.* 2(7):1–5
49. Gao Q, Yang Z, Zhu R, Wang J, Xu P, et al. 2023. Ultrasonic steering wheels: turning micromotors by localized acoustic microstreaming. *ACS Nano* 17(5):4729–39
50. Fonseca ADC, Kohler T, Ahmed D. 2022. Ultrasound-controlled swarmbots under physiological flow conditions. *Adv. Mater. Interfaces* 9(26):2200877
51. Schrage M, Medany M, Ahmed D. 2023. Ultrasound microrobots with reinforcement learning. *Adv. Mater. Technol.* 8(10):2201702
52. Ghanem MA, Maxwell AD, Wang Y-N, Cunitz BW, Khokhlova VA, et al. 2020. Noninvasive acoustic manipulation of objects in a living body. *PNAS* 117(29):16848–55
53. Lo W-C, Fan C-H, Ho Y-J, Lin C-W, Yeh C-K. 2021. Tornado-inspired acoustic vortex tweezer for trapping and manipulating microbubbles. *PNAS* 118(4):e2023188118
54. Zeng H, Wasylczyk P, Wiersma DS, Priimagi A. 2018. Light robots: bridging the gap between microrobotics and photomechanics in soft materials. *Adv. Mater.* 30(24):1703554
55. Ashkin A. 1997. Optical trapping and manipulation of neutral particles using lasers. *PNAS* 94(10):4853–60
56. Hou Y, Wang H, Fu R, Wang X, Yu J, et al. 2023. A review on microrobots driven by optical and magnetic fields. *Lab Chip* 23(5):848–68
57. Sitti M, Wiersma DS. 2020. Pros and cons: magnetic versus optical microrobots. *Adv. Mater.* 32(20):1906766
58. Kohlmeyer RR, Chen J. 2013. Wavelength-selective, IR light-driven hinges based on liquid crystalline elastomer composites. *Angew. Chemie Int. Ed.* 52(35):9234–37
59. Martella D, Paoli P, Pioner JM, Sacconi L, Coppini R, et al. 2017. Liquid crystalline networks toward regenerative medicine and tissue repair. *Small* 13(46):1702677
60. Hoang MC, Le VH, Nguyen KT, Nguyen VD, Kim J, et al. 2020. A robotic biopsy endoscope with magnetic 5-DOF locomotion and a retractable biopsy punch. *Micromachines* 11:98
61. Lim A, Schonewille A, Forbrigger C, Looi T, Drake J, Diller E. 2021. Design and comparison of magnetically-actuated dexterous forceps instruments for neuroendoscopy. *IEEE Trans. Biomed. Eng.* 68(3):846–56
62. Hu X, Yasa IC, Ren Z, Goudou SR, Ceylan H, et al. 2023. Magnetic soft micromachines made of linked microactuator networks. *Sci. Adv.* 7(23):eabe8436
63. Hong C, Ren Z, Wang C, Li M, Wu Y, et al. 2023. Magnetically actuated gearbox for the wireless control of millimeter-scale robots. *Sci. Robot.* 7(69):eabo4401
64. Nica M, Forbrigger C, Diller E. 2022. A novel magnetic transmission for powerful miniature surgical robots. *IEEE/ASME Trans. Mechatronics* 27(6):5541–50
65. Attanasio A, Scaglioni B, De Momi E, Fiorini P, Valdastrì P. 2021. Autonomy in surgical robotics. *Annu. Rev. Control Robot. Auton. Syst.* 4:651–79
66. Elfring R, de la Fuente M, Radermacher K. 2010. Assessment of optical localizer accuracy for computer aided surgery systems. *Comput. Aided Surg.* 15(1–3):1–12

67. Sorriento A, Porfido MB, Mazzoleni S, Calvosa G, Tenucci M, et al. 2020. Optical and electromagnetic tracking systems for biomedical applications: a critical review on potentialities and limitations. *IEEE Rev. Biomed. Eng.* 13:212–32
68. Franz AM, Haidegger T, Birkfellner W, Cleary K, Peters TM, Maier-Hein L. 2014. Electromagnetic tracking in medicine—a review of technology, validation, and applications. *IEEE Trans. Med. Imaging* 33(8):1702–25
69. Dam HJW. 1896. The new marvel in photography. *McClure's Mag.* 6(5):402–15
70. Flower MA. 2012. *Webb's Physics of Medical Imaging*. Boca Raton, FL: CRC Press
71. Aziz A, Pane S, Iacovacci V, Koukourakis N, Czarske J, et al. 2020. Medical imaging of microrobots: toward in vivo applications. *ACS Nano* 14(9):10865–93
72. Pane S, Zhang M, Iacovacci V, Zhang L, Menciasci A. 2022. Contrast-enhanced ultrasound tracking of helical propellers with acoustic phase analysis and comparison with color Doppler. *APL Bioeng.* 6(3):36102
73. Tiryaki ME, Sitti M. 2022. Magnetic resonance imaging-based tracking and navigation of submillimeter-scale wireless magnetic robots. *Adv. Intell. Syst.* 4(4):2100178
74. Bakenecker AC, von Gladiss A, Schwenke H, Behrends A, Friedrich T, et al. 2021. Navigation of a magnetic micro-robot through a cerebral aneurysm phantom with magnetic particle imaging. *Sci. Rep.* 11(1):14082
75. Hwang J, Jeon S, Kim B, Kim J, Jin C, et al. 2022. An electromagnetically controllable micro-robotic interventional system for targeted, real-time cardiovascular intervention. *Adv. Healthc. Mater.* 11(11):2102529
76. Go G, Yoo A, Nguyen KT, Nan M, Darmawan BA, et al. 2023. Multifunctional microrobot with real-time visualization and magnetic resonance imaging for chemoembolization therapy of liver cancer. *Sci. Adv.* 8(46):eabq8545
77. Aziz A, Holthof J, Meyer S, Schmidt OG, Medina-Sánchez M. 2021. Dual ultrasound and photoacoustic tracking of magnetically driven micromotors: from in vitro to in vivo. *Adv. Healthc. Mater.* 10(22):2101077
78. Jin D, Wang Q, Chan KF, Xia N, Yang H, et al. 2023. Swarming self-adhesive microgels enabled aneurysm on-demand embolization in physiological blood flow. *Sci. Adv.* 9(19):eadf9278
79. Pané S, Puigmartí-Luis J, Bergeles C, Chen X-Z, Pellicer E, et al. 2019. Imaging technologies for biomedical micro- and nanoswimmers. *Adv. Mater. Technol.* 4(4):1800575
80. Khalil ISM, Ferreira P, Eleutério R, De Korte CL, Misra S. 2014. Magnetic-based closed-loop control of paramagnetic microparticles using ultrasound feedback. In *Proceedings of 2014 IEEE International Conference on Robotics and Automation, Hong Kong*, pp. 3807–12. New York: IEEE
81. Šuligoj F, Heunis CM, Mohanty S, Misra S. 2022. Intravascular tracking of micro-agents using medical ultrasound: towards clinical applications. *IEEE Trans. Biomed. Eng.* 69(12):3739–47
82. Du X, Wang Q, Jin D, Chiu PWY, Pang CP, et al. 2022. Real-time navigation of an untethered miniature robot using mobile ultrasound imaging and magnetic actuation systems. *IEEE Robot. Autom. Lett.* 7(3):7668–75
83. Heunis CM, Wotte YP, Sikorski J, Furtado GP, Misra S. 2020. The ARMM system—autonomous steering of magnetically-actuated catheters: towards endovascular applications. *IEEE Robot. Autom. Lett.* 5(2):705–12
84. Wang Q, Jin D, Wang B, Xia N, Ko H, et al. 2022. Reconfigurable magnetic microswarm for accelerating tPA-mediated thrombolysis under ultrasound imaging. *IEEE/ASME Trans. Mechatron.* 27(4):2267–77
85. Faoro G, Maglio S, Pane S, Iacovacci V, Menciasci A. 2023. An artificial intelligence-aided robotic platform for ultrasound-guided transcarotid revascularization. *IEEE Robot. Autom. Lett.* 8(4):2349–56
86. Botros K, Alkhatib M, Folio D, Ferreira A. 2022. Fully automatic and real-time microrobot detection and tracking based on ultrasound imaging using deep learning. In *Proceedings 2022 International Conference on Robotics and Automation (ICRA), Philadelphia, PA*, pp. 9763–68. New York: IEEE
87. Botros K, Alkhatib M, Folio D, Ferreira A. 2023. USMicroMagSet: using deep learning analysis to benchmark the performance of microrobots in ultrasound images. *IEEE Robot. Autom. Lett.* 8(6):3254–61
88. Versluis M, Stride E, Lajoinie G, Dollet B, Segers T. 2020. Ultrasound contrast agent modeling: a review. *Ultrasound Med. Biol.* 46(9):2117–44

89. Fronheiser MP, Wolf PD, Idriss SF, Nelson RC, Lee W, Smith SW. 2004. Real-time 3D color flow Doppler for guidance of vibrating interventional devices. *Ultrason. Imaging*. 26(3):173–84
90. Fronheiser MP, Idriss SF, Wolf PD, Smith SW. 2008. Vibrating interventional device detection using real-time 3-D color Doppler. *IEEE Trans. Ultrason. Ferroelectr. Freq. Control* 55(6):1355–62
91. Singh AV, Ansari MHD, Dayan CB, Giltinan J, Wang S, et al. 2019. Multifunctional magnetic hairbot for untethered osteogenesis, ultrasound contrast imaging and drug delivery. *Biomaterials* 219:119394
92. Wang Q, Chan KF, Schweizer K, Du X, Jin D, et al. 2023. Ultrasound Doppler-guided real-time navigation of a magnetic microswarm for active endovascular delivery. *Sci. Adv.* 7(9):eabe5914
93. Wang Q, Du X, Jin D, Zhang L. 2022. Real-time ultrasound Doppler tracking and autonomous navigation of a miniature helical robot for accelerating thrombolysis in dynamic blood flow. *ACS Nano* 16(1):604–16
94. Pane S, Faoro G, Sinibaldi E, Iacovacci V, Menciassi A. 2022. Ultrasound acoustic phase analysis enables robotic visual-servoing of magnetic microrobots. *IEEE Trans. Robot.* 38(3):1571–82
95. Pane S, Iacovacci V, Sinibaldi E, Menciassi A. 2021. Real-time imaging and tracking of microrobots in tissues using ultrasound phase analysis. *Appl. Phys. Lett.* 118(1):14102
96. Pane S, Iacovacci V, Ansari MHD, Menciassi A. 2021. Ultrasound-guided navigation of a magnetic microrobot using acoustic phase analysis. *Sci. Rep.* 11:23239
97. Jensen EC. 2014. Technical review, types of imaging, part 4—magnetic resonance imaging. *Anat. Rec.* 297(6):973–78
98. Wu LC, Zhang Y, Steinberg G, Qu H, Huang S, et al. 2019. A review of magnetic particle imaging and perspectives on neuroimaging. *Am. J. Neuroradiol.* 40(2):206–12
99. Tiryaki ME, Demir SO, Sitti M. 2022. Deep learning-based 3D magnetic microrobot tracking using 2D MR images. *IEEE Robot. Autom. Lett.* 7(3):6982–89
100. Bozuyuk U, Suadiye E, Aghakhani A, Dogan NO, Lazovic J, et al. 2022. High-performance magnetic FePt (L10) surface microrollers towards medical imaging-guided endovascular delivery applications. *Adv. Funct. Mater.* 32(8):2109741
101. Nothnagel N, Rahmer J, Gleich B, Halkola A, Buzug TM, Borgert J. 2016. Steering of magnetic devices with a magnetic particle imaging system. *IEEE Trans. Biomed. Eng.* 63(11):2286–93
102. Bruker Corp. 2023. Preclinical magnetic particle imaging (MPI) scanner. <https://www.bruker.com/it/products-and-solutions/preclinical-imaging/mpi.html>
103. Rahmer J, Stehning C, Gleich B. 2018. Remote magnetic actuation using a clinical scale system. *PLOS ONE* 13(3):e0193546
104. Wilhelm S, Tavares AJ, Dai Q, Ohta S, Audet J, et al. 2016. Analysis of nanoparticle delivery to tumours. *Nat. Rev. Mater.* 1(5):16014
105. Schuerle S, Soleimany AP, Yeh T, Anand GM, Häberli M, et al. 2019. Synthetic and living micropropellers for convection-enhanced nanoparticle transport. *Sci. Adv.* 5(4):eaav4803
106. Xin C, Jin D, Hu Y, Yang L, Li R, et al. 2021. Environmentally adaptive shape-morphing microrobots for localized cancer cell treatment. *ACS Nano* 15(11):18048–59
107. Alapan Y, Bozuyuk U, Erkoç P, Karacakol AC, Sitti M. 2020. Multifunctional surface microrollers for targeted cargo delivery in physiological blood flow. *Sci. Robot.* 5(42):eaba5726
108. Miki K, Clapham DE. 2013. Rheotaxis guides mammalian sperm. *Curr. Biol.* 23(6):443–52
109. Kaupp UB, Strücker T. 2017. Signaling in sperm: more different than similar. *Trends Cell Biol.* 27(2):101–9
110. Ahmed D, Baasch T, Blondel N, Läubli N, Dual J, Nelson BJ. 2017. Neutrophil-inspired propulsion in a combined acoustic and magnetic field. *Nat. Commun.* 8(1):770
111. Ahmed D, Sukhov A, Hauri D, et al. 2021. Bioinspired acousto-magnetic microswarm robots with upstream motility. *Nat. Mach. Intell.* 3:116–124
112. Bozuyuk U, Alapan Y, Aghakhani A, Yunusa M, Sitti M. 2021. Shape anisotropy-governed locomotion of surface microrollers on vessel-like microtopographies against physiological flows. *PNAS* 118(13):e2022090118
113. Del Campo Fonseca A, Glück C, Droux J, Ferry Y, Frei C, et al. 2023. Ultrasound trapping and navigation of microrobots in the mouse brain vasculature. *Nat. Commun.* 14(1):5889

114. Pancaldi L, Dirix P, Fanelli A, Lima AM, Stergiopoulos N, et al. 2020. Flow driven robotic navigation of microengineered endovascular probes. *Nat. Commun.* 11(1):6356
115. Kim Y, Genevriere E, Harker P, Choe J, Balicki M, et al. 2022. Telerobotic neurovascular interventions with magnetic manipulation. *Sci. Robot.* 7(65):eabg9907
116. Rivkin B, Becker C, Singh B, Aziz A, Akbar F, et al. 2023. Electronically integrated microcatheters based on self-assembling polymer films. *Sci. Adv.* 7(51):eabl5408
117. Gopesh T, Wen JH, Santiago-Dieppa D, Yan B, Pannell JS, et al. 2021. Soft robotic steerable microcatheter for the endovascular treatment of cerebral disorders. *Sci. Robot.* 6(57):eabf0601
118. Leber A, Dong C, Laperrousaz S, Banerjee H, Abdelaziz MEMK, et al. 2023. Highly integrated multi-material fibers for soft robotics. *Adv. Sci.* 10(2):2204016
119. Ciuti G, Skonieczna-Żydecka K, Marlicz W, Iacovacci V, Liu H, et al. 2020. Frontiers of robotic colonoscopy: a comprehensive review of robotic colonoscopes and technologies. *J. Clin. Med.* 9(6):1648
120. Li S, Liu D, Hu Y, Su Z, Zhang X, et al. 2022. Soft magnetic microrobot doped with porous silica for stability-enhanced multimodal locomotion in a nonideal environment. *ACS Appl. Mater. Interfaces* 14(8):10856–74
121. Wang C, Mzyk A, Schirhagl R, Misra S, Venkiteswaran VK. 2023. Biocompatible film-coating of magnetic soft robots for mucoadhesive locomotion. *Adv. Mater. Technol.* 8(12):2201813
122. Wu Y, Dong X, Kim J, Wang C, Sitti M. 2023. Wireless soft millirobots for climbing three-dimensional surfaces in confined spaces. *Sci. Adv.* 8(21):eabn3431
123. Abramson A, Caffarel-Salvador E, Khang M, Dellal D, Silverstein D, et al. 2019. An ingestible self-orienting system for oral delivery of macromolecules. *Science* 363(6427):611–15
124. Qin Y, Cai Z, Han J. 2023. Design and control of a magnetically-actuated anti-interference microrobot for targeted therapeutic delivery. *IEEE Robot. Autom. Lett.* 8(9):5672–79
125. Yang Q, Tang S, Lu D, Li Y, Wan F, et al. 2022. Pollen typhae-based magnetic-powered microrobots toward acute gastric bleeding treatment. *ACS Appl. Bio Mater.* 5(9):4425–34
126. Huang C, Lai Z, Wu X, Xu T. 2022. Multimodal locomotion and cargo transportation of magnetically actuated quadruped soft microrobots. *Cyborg Bionic Syst.* 2022:0004
127. Wang C, Wu Y, Dong X, Armacki M, Sitti M. 2023. In situ sensing physiological properties of biological tissues using wireless miniature soft robots. *Sci. Adv.* 9(23):eadg3988
128. Zhang C, Pan C, Chan KF, Gao J, Yang Z, et al. 2023. Wirelessly powered deformable electronic stent for noninvasive electrical stimulation of lower esophageal sphincter. *Sci. Adv.* 9(10):eade8622
129. Soon RH, Yin Z, Dogan MA, Dogan NO, Tiryaki ME, et al. 2023. Pangolin-inspired untethered magnetic robot for on-demand biomedical heating applications. *Nat. Commun.* 14(1):3320
130. Xu Z, Wu Z, Yuan M, Chen H, Ge W, Xu Q. 2023. Multiple cilia-like swarms enable efficient microrobot deployment and execution. *Cell Rep. Phys. Sci.* 4(3):101329
131. Jeon S, Kim S, Ha S, Lee S, Kim E, et al. 2019. Magnetically actuated microrobots as a platform for stem cell transplantation. *Sci. Robot.* 4(30):eaav4317
132. Forbrigger C, Fredin E, Diller E. 2023. Evaluating the feasibility of magnetic tools for the minimum dynamic requirements of microneurosurgery. In *2023 IEEE International Conference on Robotics and Automation (ICRA), London, United Kingdom*, pp. 4703–9. New York: IEEE
133. Dogangil G, Ergeneman O, Abbott JJ, Pane S, Hall H, et al. 2008. Toward targeted retinal drug delivery with wireless magnetic microrobots. In *2008 IEEE/RSJ International Conference on Intelligent Robots and Systems, Nice, France*, pp. 1921–26. New York: IEEE
134. Kim M-S, Lee H-T, Ahn S-H. 2019. Laser controlled 65 micrometer long microrobot made of Ni-Ti shape memory alloy. *Adv. Mater. Technol.* 4(12):1900583
135. Charreyron SL, Boehler Q, Danun AN, Mesot A, Becker M, Nelson BJ. 2021. A magnetically navigated microcannula for subretinal injections. *IEEE Trans. Biomed. Eng.* 68(1):119–29
136. Pittiglio G, Lloyd P, da Veiga T, Onaizah O, Pompili C, et al. 2022. Patient-specific magnetic catheters for atraumatic autonomous endoscopy. *Soft Robot.* 9(6):1120–33
137. Phelan MF III, Tiryaki ME, Lazovic J, Gilbert H, Sitti M. 2022. Heat-mitigated design and Lorentz force-based steering of an MRI-driven microcatheter toward minimally invasive surgery. *Adv. Sci.* 9(10):2105352

138. Wang Q, Yu J, Yuan K, Yang L, Jin D, Zhang L. 2020. Disassembly and spreading of magnetic nanoparticle clusters on uneven surfaces. *Appl. Mater. Today* 18:100489
139. Casagrande G, Ibrahim M, Semproni F, Iacovacci V, Menciassi A. 2022. Hydraulic detrusor for artificial bladder active voiding. *Soft Robot.* 10(2):269–79
140. Rajabasadi F, Moreno S, Fichna K, Aziz A, Appelhans D, et al. 2022. Multifunctional 4D-printed sperm-hybrid microcarriers for assisted reproduction. *Adv. Mater.* 34(50):2204257
141. Schwarz L, Karnaushenko DD, Hebenstreit F, Naumann R, Schmidt OG, Medina-Sánchez M. 2020. A rotating spiral micromotor for noninvasive zygote transfer. *Adv. Sci.* 7(18):2000843
142. Llacer-Wintle J, Rivas-Dapena A, Chen X-Z, Pellicer E, Nelson BJ, et al. 2021. Biodegradable small-scale swimmers for biomedical applications. *Adv. Mater.* 33(42):2102049
143. Iacovacci V, Ricotti L, Sinibaldi E, Signore G, Vistoli F, Menciassi A. 2018. An intravascular magnetic catheter enables the retrieval of nanoagents from the bloodstream. *Adv. Sci.* 5(9):1800807
144. Faoro G, Iacovacci V, Menciassi A. 2024. Optical flow and acoustic phase analysis comparison in ultrasound-based microrobot tracking. *IEEE Robot. Autom. Lett.* 9(2):1985–92
145. Yip M, Salcudean S, Goldberg K, Althoefer K, Menciassi A, et al. 2023. Artificial intelligence meets medical robotics. *Science* 381(6654):141–46
146. Pore A, Li Z, Dall'Alba D, Hernansanz A, De Momi E, et al. 2023. Autonomous navigation for robot-assisted intraluminal and endovascular procedures: a systematic review. *IEEE Trans. Robot.* 39(4):2529–48

